Photonic Implementations of Continuous Variable Quantum Computing with Gottesman-Kitaev-Preskill codes

Haochen (Paul) Wang
wangh274, 1004715114

Term Paper, PHY2204 Quantum Optics 2
University of Toronto, Winter 2024

Abstract

A promising candidate for the physical implementation of a quantum computer is a photonic quantum computer encoded in oscillator states of light. Not only does it require only room temperature instead of cryogenic temperatures, but with the now-matured Gottesman-Kitaev-Preskill (GKP) encoding, it also has adequate support for error correction and thus is in principle scalable [1]. More importantly, with GKP encoding, qubit Clifford operations map to continuous variable (CV) Gaussian operations, which can be implemented deterministically and easily using linear optical elements, homodyne detection, and Gaussian states of light [2]. In addition, the technology for producing GKP states has also matured in the past few years, using the technique of Gaussian Boson Sampling (GBS) [3, 4, 5]. Here, we provide a tutorial-style literature review of these topics, specifically on the physical implementation of GKP gates and production of GKP states. The review is geared towards someone with a standard quantum physics background, interested in learning about photonic quantum computing.

Contents

1 Introduction

For many students of quantum computing, one inevitable wonder they would have during their studies is, how one could actually implement a quantum computer in the lab. While the abstract qubit model offers great insights into the workings of various interesting quantum algorithms, it tells us nothing about the actual physical implementation. Many standard texts on the subject, such as that of Nielson and Chuang [6], only touches briefly, if even at all, on the physical implementation. On the other hand, there has been considerable progress on building the hardware of quantum computers over the past few decades [1, 2, 3, 4, 5, 7]. However, outside of the academic papers themselves, there is little to no educational resource on these materials.

This paper aims to bridge this gap, specifically for the photonic implementation scheme of quantum computers. We review and present the current methodologies used in photonic quantum computing.

Section 2 will review the so-called "continuous-variable" (CV) quantum mechanics. This is nothing but a fancy name for the quantum mechanics of light, or the quantum mechanics of harmonic oscillators. There are many well-received texts on quantum optics [8, 9]. We will present the bare essentials necessary for understanding photonic quantum computers. After that, we will look at how the various operations on light states can be implemented physically in the lab, using only optical components.

Section 3 will introduce the Gottesman-Kitaev-Preskill (GKP) encoding [1]. At a high-level, the GKP encoding is a design that maps some specific light state to the logical zero qubit, and some other specific light state to the logical one qubit. These light states will be referred to as GKP states. We will examine this mapping, and look at how the various Clifford qubit operations can be achieved simply by the corresponding Gaussian operations on light. For example, we will find that the Hadamard gate is simply a rotation of $\pi/2$ in phase space, or in other words just a phase shifter!

Section 4 will look at how the GKP states can be physically produced. The method involved, Gaussian Boson Sampling (GBS) [10], utilizes entanglement to essentially prepare *any* light state we wish. This preparation is probabilistic due to the quantum nature of entanglement, but recent progress has been made on achieving good production probability [4, 5].

2 Implementation of Basic CV Operations

2.1 Overview of Continuous Variable Quantum Optics

The reader is assumed to have decent familiarity of the topics discussed in this section.

2.1.1 The Quadrature Variables

The electromagnetic fields that constitute light is a linear superposition of different modes, with each mode having a distinct combination of a frequency and a polarization. When one calculates the total energy of the electromagnetic fields, one finds that the total Hamiltonian is the sum of the Hamiltonians of all the individual modes, with the Hamiltonian of an individual mode being the Hamiltonian of a harmonic oscillator (with unit mass) whose frequency is that of the mode [8]. Hence, the overall Hilbert space for light is the tensor product of all the Hilbert spaces of the individual modes.

For a single mode k with frequency ω_k, the Hamiltonian is

$$\hat{H}_k = \hbar\omega_k(\hat{a}_k^\dagger \hat{a}_k + \frac{1}{2}) = \frac{1}{2}(\hat{p}_k^2 + \omega_k^2 \hat{x}_k^2) \tag{1}$$

where the (dimensionful) position and momentum operators

$$\hat{x}_k = \sqrt{\frac{\hbar}{2\omega_k}}(\hat{a}_k + \hat{a}_k^\dagger) \tag{2}$$

$$\hat{p}_k = -i\sqrt{\frac{\hbar\omega_k}{2}}(\hat{a}_k - \hat{a}_k^\dagger) \tag{3}$$

satisfy the usual commutation relation

$$[\hat{x}_k,\, \hat{p}_{k'}] = i\hbar\, \delta_{kk'} \tag{4}$$

and the (dimensionless) creation and annihilation operations satisfy the usual bosonic commutation relation

$$[\hat{a}_k, \hat{a}_{k'}^\dagger] = \delta_{kk'} \tag{5}$$

$$[\hat{a}_k, \hat{a}_{k'}] = [\hat{a}_k^\dagger, \hat{a}_{k'}^\dagger] = 0 \tag{6}$$

In quantum optics, it is standard practice to work with the *dimensionless* pair of conjugate variables, the so-called position and momentum "quadratures", defined by taking the real

and imaginary parts of $\hat{a}_k$:

$$\hat{X}_k = \mathrm{Re}\,\hat{a}_k = \sqrt{\frac{\omega_k}{2\hbar}}\,\hat{x}_k \tag{7}$$

$$\hat{P}_k = \mathrm{Im}\,\hat{a}_k = \sqrt{\frac{1}{2\hbar\omega_k}}\,\hat{p}_k \tag{8}$$

The creation and annihilation operators and the quadrature operators are thus related via

$$\hat{a}_k = \hat{X}_k + i\hat{P}_k\,, \qquad \hat{a}_k^\dagger = \hat{X}_k - i\hat{P}_k \tag{9}$$

$$\hat{X}_k = \frac{1}{2}(\hat{a}_k + \hat{a}_k^\dagger)\,, \quad \hat{P}_k = \frac{1}{2i}(\hat{a}_k - \hat{a}_k^\dagger) \tag{10}$$

The commutation relations also reduce to the dimensionless form

$$[\hat{X}_k, \hat{P}_{k'}] = \frac{i}{2}\,\delta_{kk'} \tag{11}$$

(Colloquially, some people call this the "$\hbar = 1/2$ convention".)

What do these quadratures represent? Consider the electric field of a single mode (for a single polarization) [1][8]

$$\hat{E}_k(\mathbf{r}, t) = E_0\,[\hat{a}_k\, e^{i(\mathbf{k}\cdot\mathbf{r}-\omega_k t)} + \hat{a}_k^\dagger\, e^{-i(\mathbf{k}\cdot\mathbf{r}-\omega_k t)}] \tag{12}$$

$$= E_0[(\hat{X}_k + i\hat{P}_k)\, e^{i(\mathbf{k}\cdot\mathbf{r}-\omega_k t)} + \text{c.c.}] \tag{13}$$

$$= 2E_0[\hat{X}_k \cos(\omega_k t - \mathbf{k}\cdot\mathbf{r}) + \hat{P}_k \sin(\omega_k t - \mathbf{k}\cdot\mathbf{r})] \tag{14}$$

We let E_0 to be the field amplitude carrying all the dimensions. "c.c." stand for "complex conjugate", or "hermitian conjugate" when appropriate.

We see that the position and momentum quadrature of a mode represent the in-phase and out-of-phase components of the electric field amplitude of the mode, with respect to some reference wave $\cos(\omega_k t - \mathbf{k}\cdot\mathbf{r})$. The phase of this reference wave, or the phase of the states, is of course arbitrary, and this leads us to define the more general pair of quadratures

$$\hat{X}_k^{(\theta)} = \frac{1}{2}(\hat{a}_k e^{-i\theta} + \hat{a}_k^\dagger e^{i\theta}) \tag{15}$$

$$\hat{P}_k^{(\theta)} = \frac{1}{2i}(\hat{a}_k e^{-i\theta} - \hat{a}_k^\dagger e^{i\theta}) \tag{16}$$

[1]The form of the electric field operator is obtained by the standard quantization recipe: write down the classical electric field from Maxwell's equations, and promote observables to operators. We assume the reader is familiar with such procedures.

They are related to the "old" quadratures by a phase space rotation of angle θ:

$$\begin{pmatrix} \hat{X}_k^{(\theta)} \\ \hat{P}_k^{(\theta)} \end{pmatrix} = \begin{pmatrix} \cos\theta & \sin\theta \\ -\sin\theta & \cos\theta \end{pmatrix} \begin{pmatrix} \hat{X}_k \\ \hat{P}_k \end{pmatrix} \tag{17}$$

Since the two sets of quadratures are related via a unitary, they share the same commutation relations. In other words, the bosonic commutator $[\hat{X}_k^{(\theta)}, \hat{P}_k^{(\theta)}] = i\delta_{kk'}/2$ still holds, and the new phase-ful quadratures are a pair of valid conjugate variables.

With these general-phase quadrature operators, the electric field operator becomes

$$\hat{E}_k(\mathbf{r}, t) = 2E_0[\hat{X}_k^{(\theta)} \cos(\omega_k t - \mathbf{k}\cdot\mathbf{r} - \theta) + \hat{P}_k^{(\theta)} \sin(\omega_k t - \mathbf{k}\cdot\mathbf{r} - \theta)] \tag{18}$$

and we have changed the phase of the reference wave.

A useful realization from equation (15) is that the zero-phase momentum quadrature is simply the position quadrature delayed by $\pi/2$ in phase:

$$\hat{X}_k^{(\theta=\pi/2)} = \frac{1}{2}(-i\hat{a}_k + i\hat{a}_k^\dagger) = \frac{1}{2i}(\hat{a}_k - \hat{a}_k^\dagger) = \hat{P}_k \tag{19}$$

This is in fact true for all phases, i.e. $\hat{X}_k^{(\theta+\pi/2)} = \hat{P}_k^{(\theta)}$. This insight will prove convenient when we try to measure the quadratures.

2.1.2 The Wigner Function

Let (x, p) be the phase space coordinates (for the zero-phase quadrature operators $\hat{X}, \hat{P}$), where we have now dropped the subscript k when it is understood that we are talking about the single-mode field. The Wigner function that describes the phase space statistics of a (pure) quantum state ψ of the oscillator is defined as

$$W_\psi(x, p) = \frac{1}{2\pi}\int_{-\infty}^{\infty} dx' e^{ipx'}\, \psi^*(x + \frac{x'}{2})\, \psi(x - \frac{x'}{2}) \tag{20}$$

where $\psi(x) = \langle x|\psi\rangle$ is the state's wavefunction in the position basis.

For an oscillator state, the Wigner function evolves in time by simply rotating clockwise, *with no distortion whatsoever* [11]. It is also worth noting that for a superposition state $|\psi_1\rangle + |\psi_2\rangle$, the Wigner function is **not** simply $W_{\psi_1}(x, p) + W_{\psi_2}(x, p)$, as there will be cross terms in the integrand of (20).

2.1.3 Single-Mode Operations

The effect of a single-mode operation on the quadrature operators can be easily seen in the Heisenberg picture. If we imagine the quadrature operators $(\hat{X}, \hat{P})$, and consequently $\hat{a} = \hat{X} + i\hat{P}$, to carry the dynamics of a system, then the evolution under some unitary operation $\hat{U}$ is easily given by

$$\hat{a}' = \hat{U}^\dagger \, \hat{a} \, \hat{U} \tag{21}$$

where the system before the unitary is unprimed, and system after is primed, since $\langle\psi|\hat{a}'|\psi\rangle = \langle\psi|\hat{U}^\dagger\hat{a}\hat{U}|\psi\rangle$.

For example, the effect of the displacement operator $\hat{D}(\alpha) = \exp\big(\alpha\hat{a}^\dagger - \alpha^*\hat{a}\big)$ can be read off from

$$\hat{a}' = \hat{D}^\dagger(\alpha) \, \hat{a} \, \hat{D}(\alpha) = \hat{a} + \alpha \tag{22}$$

Casting the ladder operator back to quadratures:

$$\hat{X}' + i\hat{P}' = \hat{X} + i\hat{P} + \alpha \tag{23}$$

Taking and real and imaginary parts:

$$\hat{X}' = \hat{X} + \operatorname{Re}\alpha, \quad \hat{P}' = \hat{P} + \operatorname{Im}\alpha \tag{24}$$

We we see indeed the effect of the displacement operator $\hat{D}(\alpha)$ on the quadrature operators is a complex displacement of α.

Equations like (22) are calculated from the operator expansion theorem. We will delegate all such calculations to Appendix A.

2.1.4 Optical Devices as Input-Output Devices

In general, an optical device is a device that takes in n input modes and produces n output modes, relating them by some unitary $\hat{U}$. We can represent an optical device via the following generalized optical circuit symbol in figure 1.

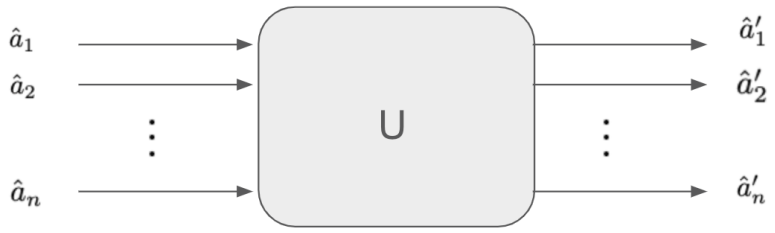

Figure 1: A general optical device with input modes $\hat{a}_i$ and output modes $\hat{a}'_i$.

The input and output modes are related via

$$\begin{pmatrix} \hat{a}'_1 \\ \hat{a}'_2 \\ \vdots \\ \hat{a}'_n \end{pmatrix} = U \begin{pmatrix} \hat{a}_1 \\ \hat{a}_2 \\ \vdots \\ \hat{a}_n \end{pmatrix} \tag{25}$$

or, $\hat{a}'_i = \sum_j U_{ij}\, \hat{a}_j$, $\hat{a}^{\dagger\prime}_i = \sum_j U_{ij}{}^*\, \hat{a}^\dagger_j$.

The matrix U must be unitary to preserve the bosonic commutator between the output modes:

$$\begin{aligned} \left[\hat{a}'_i, \hat{a}^{\dagger\prime}_j\right] &= \left[\sum_k U_{ik}\hat{a}_k\,,\, \sum_p U_{jp}{}^*\hat{a}^\dagger_p\right] \\ &= \sum_{kp} U_{ik}U_{jp}{}^* \underbrace{\left[\hat{a}_k, \hat{a}^\dagger_p\right]}_{\delta_{kp}} \\ &= \sum_k U_{ik}U_{jk}{}^* \\ &= \delta_{ij} \end{aligned} \tag{26}$$

When there is only one input mode and one output mode, this device reduces to the single-mode operations discussed in the previous section. This is also why in the previous section, we restricted single-mode operations to be unitary.

A very common two-port optical device is the beam-splitter. For a in-depth discussion of the beam-splitter, refer to standard quantum optics texts [8].

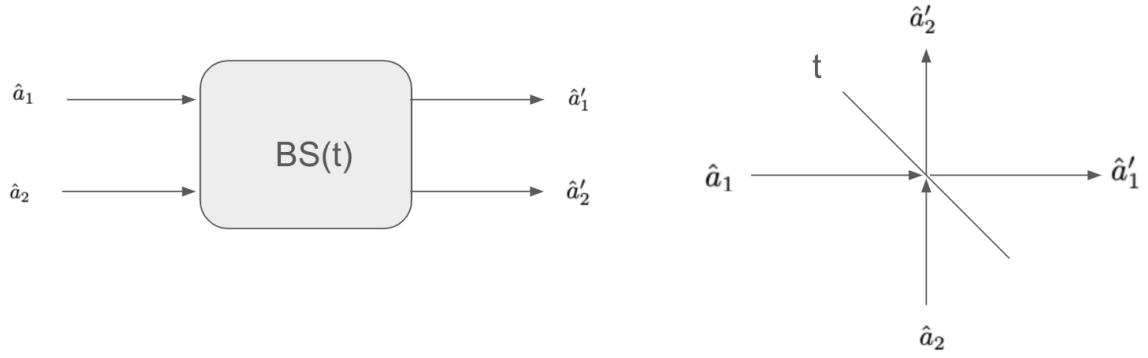

Figure 2: A beam splitter with transmission coefficient t, in the general optical device schematic (left) and the traditional schematic (right) highlighting the transmission/reflection relationships.

With transmission coefficient t and reflection coefficient r, the input/output modes are related via

$$\begin{pmatrix} \hat{a}'_1 \\ \hat{a}'_2 \end{pmatrix} = \begin{pmatrix} t & r \\ r & t \end{pmatrix} \begin{pmatrix} \hat{a}_1 \\ \hat{a}_2 \end{pmatrix} \tag{27}$$

Demanding the matrix to be unitary, we arrive at

$$|t|^2 + |r|^2 = 1, \;\; tr^* + rt^* = 0 \tag{28}$$

which is the correct Stokes relations for transmissive and reflective optical entities.

2.2 The Phase Shifter

Now that we have a well-defined meaning for the phase of a state, we can easily implement a phase shifter. To change the phase θ of the state, equation (17) instructs us to perform a rotation on the state by θ in phase space. One very straightforward way of achieving this is simple time evolution, as the time evolution of the Wigner function of an oscillator is just a rotation in phase space [11]. To achieve simple time evolution, a phase shifter can be as simple as just a length of optical fibre [8, p.143], so that the light takes some more time to travel in the circuit before reaching the next circuit component, causing a phase shift.

In equation (18), from the form of the reference wave $\cos(\omega t - \theta)$ (we drop the $\mathbf{k}\cdot\mathbf{r}$ here), we see that changing the phase via time evolution amounts to the simple rewrite $\cos(\omega t - \theta) = \cos(\omega(t - \theta/\omega))$. The other rewrite, namely $\cos(\omega t - \theta) = \cos(t(\omega - \theta/t))$, suggests that a phase shift can also be implemented by adjusting the oscillator frequency. A particular implementation in this approach is known as a thermo-optic phase shifter, which is a (sometimes curved) waveguide that changes properties when heated up using a resistor [12].

The phase space operator for a phase shift is simply a rotation:

$$\hat{R}(\theta) = \exp\left(i\theta\hat{a}^\dagger\hat{a}\right) \tag{29}$$

Its effects on the quadratures are given by (Appendix A)

$$\hat{R}^\dagger(\theta)\,\hat{a}\,\hat{R}(\theta) = \hat{a}e^{i\theta} \tag{30}$$

which is a rotation indeed.

The circuit symbol is simply one component, since the physical implementation, either with a length of optical fibre or thermo-optical heating, involves just one module.

Figure 3: Optical circuit symbol for a phase shifter.

2.3 Quadrature Measurement

Surprisingly, with just the phase shifter and the beam splitter, we can already measure the quadrature operators. This scheme is the famous homodyne detection [2, 7, 8] [2]. In the homodyne detection scheme, we use an assisting coherent state $|\beta\rangle$ and send it into a 50-50 beam splitter, together with the to-be-measured state $|\psi\rangle$. Then we measure the difference in the photon counts at the output ports of the beam splitter. Figure 4 illustrates the optical circuit for homodyne detection.

[2] "Homodyne" means "using a reference state of the same frequency".

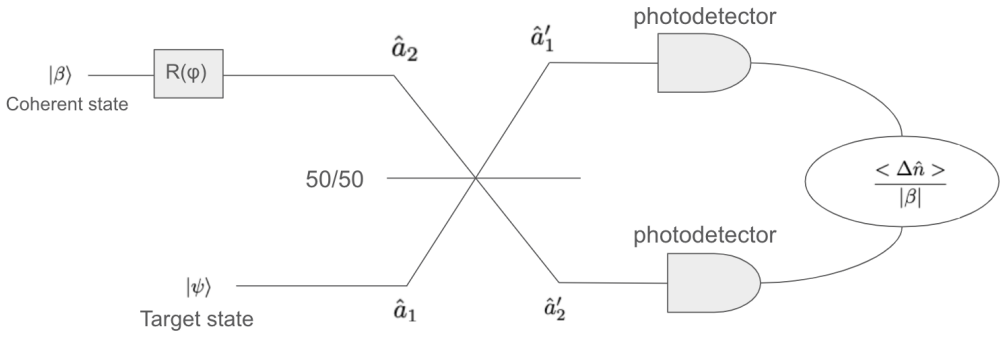

Figure 4: Optical circuit for homodyne detection. $|\psi\rangle$ is the state to be measured, $|\beta\rangle$ is a coherent state. The measured quantity is the difference between the two photocurrents.

For the 50-50 beam splitter, the reflected and transmitted amplitudes are the same. Based on the Stokes relations (28), we can pick $t = 1/\sqrt{2}, r = i/\sqrt{2}$, so $\hat{a}'_1 = (\hat{a}_1 + i\hat{a}_2)/\sqrt{2}$, $\hat{a}'_2 = (\hat{a}_2 + i\hat{a}_1)/\sqrt{2}$.

A photodetector is a device that produces a current proportional to the amount of light, or number of photons, that it detects. The measured quantity is the difference of the photocurrents, hence the difference of the number of photons.

$$\hat{n}'_1 = \hat{a}_1^{\dagger\prime}\hat{a}'_1 = \frac{1}{2}(\hat{a}_1^\dagger - i\hat{a}_2^\dagger)(\hat{a}_1 + i\hat{a}_2) = \frac{1}{2}(\hat{a}_1^\dagger\hat{a}_1 - i\hat{a}_2^\dagger\hat{a}_1 + i\hat{a}_1^\dagger\hat{a}_2 + \hat{a}_2^\dagger\hat{a}_2) \tag{31}$$

$$\hat{n}'_2 = (\hat{n}'_1 \text{ but with } \hat{a}_1 \text{ and } \hat{a}_2 \text{ reversed}) = \frac{1}{2}(\hat{a}_2^\dagger\hat{a}_2 - i\hat{a}_1^\dagger\hat{a}_2 + i\hat{a}_2^\dagger\hat{a}_1 + \hat{a}_1^\dagger\hat{a}_1) \tag{32}$$

$$\Delta\hat{n} = \hat{n}'_1 - \hat{n}'_2 = i(\hat{a}_1^\dagger\hat{a}_2 - \hat{a}_2^\dagger\hat{a}_1) \tag{33}$$

Notice $\Delta\hat{n}$ is Hermitian, as expected. When we measure the difference of the photocurrents, we are effectively measuring $\langle\Delta\hat{n}\rangle$. Since we have arranged $\Delta\hat{n}$ in terms of mode 1 and 2, we can now take the expectation with the states $|\psi\rangle$ and $|\beta\rangle$ in these modes.

$$\begin{aligned}\langle\Delta\hat{n}\rangle &= i[\,\langle\psi|\hat{a}_1^\dagger|\psi\rangle\ \langle\beta|\hat{a}_2|\beta\rangle - \langle\beta|\hat{a}_2^\dagger|\beta\rangle\ \langle\psi|\hat{a}_1|\psi\rangle\,] \\ &= i[\,\beta\,\langle\psi|\hat{a}_1^\dagger|\psi\rangle - \beta^*\,\langle\psi|\hat{a}_1|\psi\rangle\,]\end{aligned} \tag{34}$$

where we used $\hat{a}\,|\beta\rangle = \beta\,|\beta\rangle$, i.e. coherent states are annihilation eigenstates.

Denote $\beta = |\beta|e^{i\phi}$. Thus

$$\begin{aligned}\langle\Delta\hat{n}\rangle &= i|\beta|\,[e^{i\phi}\,\langle\psi|\hat{a}_1^\dagger|\psi\rangle - e^{-i\phi}\,\langle\psi|\hat{a}_1|\psi\rangle] \\ &= |\beta|\,[e^{i(\phi+\pi/2)}\,\langle\psi|\hat{a}_1^\dagger|\psi\rangle + e^{-i(\phi+\pi/2)}\,\langle\psi|\hat{a}_1|\psi\rangle]\end{aligned} \tag{35}$$

Comparing (35) and (15), we see that $\langle \Delta \hat{n} \rangle \propto \langle \psi | \hat{X}^{(\phi+\pi/2)} | \psi \rangle$. In other words, measuring the difference in the photocurrents amounts to measuring the position quadrature of the state $|\psi\rangle$! By adjusting the phase ϕ of the coherent state $|\beta\rangle$, we can effectively measure the position quadrature of any phase. This adjustment of the coherent state $|\beta\rangle$ can simply be done by inserting a phase shifter after it, as seen in figure 4.

If we wish to measure the momentum quadrature $\hat{P}^{(\theta)}$, our realization from equation (19) tells us that this is equivalent to measuring $\hat{X}^{(\theta+\pi/2)}$, so the momentum measurement can be subsumed into the same scheme as the position measurement.

2.4 Displacement Operator

We now move on to discuss how some other common single-mode phase space operators can be implemented with optical elements. The first of these operators is the displacement operator $\hat{D}(\alpha) = \exp\left(\alpha \hat{a}^\dagger - \alpha^* \hat{a}\right)$. It can be implemented with the help of an almost-transparent beam splitter and a highly-excited coherent state [13]. Figure 6 shows the optical circuit for displacing an input state $|\psi\rangle$.

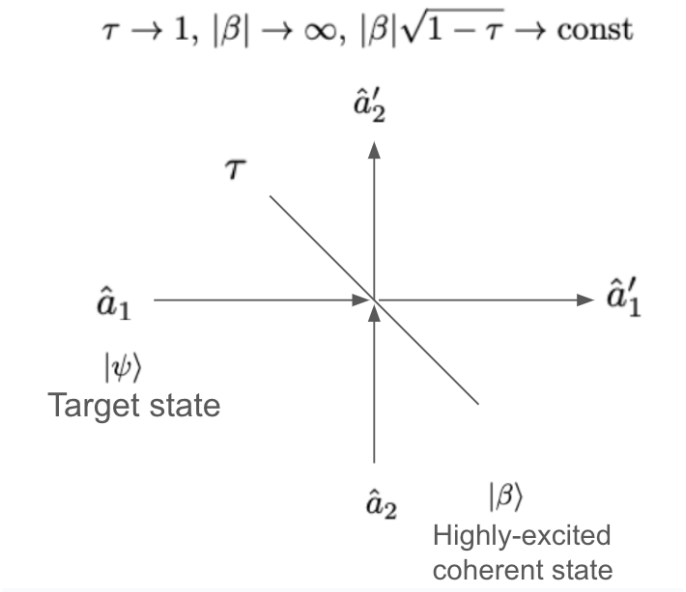

Figure 5: Optical circuit for the displacement operator. $|\psi\rangle$ is the state to be displaced, $|\beta\rangle$ is a highly-excited coherent state. The transmission and reflection coefficients of the beam splitter are $\sqrt{\tau}$ and $i\sqrt{1-\tau}$, respectively. The output state at port $\hat{a}_1'$ is the displaced state $\hat{D}(i\beta\sqrt{1-\tau})\,|\psi\rangle$.

The transmission and reflection coefficients of the beam splitter, $t = \sqrt{\tau}$ and $r = i\sqrt{1-\tau}$, satisfy the Stokes relations (28). The input and output modes are related via

$$\begin{pmatrix} \hat{a}_1' \\ \hat{a}_2' \end{pmatrix} = \begin{pmatrix} \sqrt{\tau} & i\sqrt{1-\tau} \\ i\sqrt{1-\tau} & \sqrt{\tau} \end{pmatrix} \begin{pmatrix} \hat{a}_1 \\ \hat{a}_2 \end{pmatrix}, \begin{pmatrix} \hat{a}_1 \\ \hat{a}_2 \end{pmatrix} = \begin{pmatrix} \sqrt{\tau} & -i\sqrt{1-\tau} \\ -i\sqrt{1-\tau} & \sqrt{\tau} \end{pmatrix} \begin{pmatrix} \hat{a}_1' \\ \hat{a}_2' \end{pmatrix} \tag{36}$$

The input state is

$$\begin{aligned} |\psi\rangle_1 |\beta\rangle_2 &= (\frac{1}{\pi} \int d^2\alpha \, |\alpha\rangle_1 \langle\alpha|\psi\rangle) (\hat{D}_2(\beta) |0\rangle_2) \\ &= \frac{1}{\pi} \int d^2\alpha \, \langle\alpha|\psi\rangle \, \hat{D}_1(\alpha)\hat{D}_2(\beta) |0\rangle_1 |0\rangle_2 \end{aligned} \tag{37}$$

where we used the coherent states as a overcomplete basis $\int d^2\alpha \, |\alpha\rangle \langle\alpha| = \pi$ [8], and we drop the "mode 1" subscript on the inner product $\langle\alpha|\psi\rangle$ since it's just a number and not a state vector. The mode 2 displacement operator can be rewritten with the primed output modes with the Baker–Campbell–Hausdorff (BCH) formula:

$$\begin{aligned} \hat{D}_2(\beta) &= \exp\Big(\beta\hat{a}_2^\dagger - \beta^*\hat{a}_2\Big) = \exp\Big[\beta(i\sqrt{1-\tau}\hat{a}_1^{\dagger\prime} + \sqrt{\tau}\hat{a}_2^{\dagger\prime}) - \beta^*(-i\sqrt{1-\tau}\hat{a}_1' + \sqrt{\tau}\hat{a}_2')\Big] \\ &= \exp\Big[(i\beta\sqrt{1-\tau})\hat{a}_1^{\dagger\prime} - (i\beta\sqrt{1-\tau})^* \, \hat{a}_1' + (\beta\sqrt{\tau})\hat{a}_2^{\dagger\prime} - (\beta\sqrt{\tau})^* \, \hat{a}_2'\Big] \\ &= \exp\Big[(i\beta\sqrt{1-\tau})\hat{a}_1^{\dagger\prime} - (i\beta\sqrt{1-\tau})^* \, \hat{a}_1'\Big] \, \exp\Big[(\beta\sqrt{\tau})\hat{a}_2^{\dagger\prime} - (\beta\sqrt{\tau})^* \, \hat{a}_2'\Big] \\ &= \hat{D}_1'(i\beta\sqrt{1-\tau}) \, \hat{D}_2'(\beta\sqrt{\tau}) \end{aligned} \tag{38}$$

since the BCH formula reduces to $e^{\hat{A}+\hat{B}} = e^{\hat{A}}e^{\hat{B}}$ when $[\hat{A}, \hat{B}] = 0$, and operators across different modes commute. A similar calculation, or the previous one with the roles of mode 1 and 2 swapped, shows that $\hat{D}_1(\alpha) = \hat{D}_1'(\alpha\sqrt{\tau}) \, \hat{D}_2'(i\alpha\sqrt{1-\tau})$. The input state (37) is thus rewritten as the output state

$$\frac{1}{\pi} \int d^2\alpha \, \langle\alpha|\psi\rangle \, \hat{D}_1'(\alpha\sqrt{\tau}) \, \hat{D}_2'(i\alpha\sqrt{1-\tau}) \, \hat{D}_1'(i\beta\sqrt{1-\tau}) \, \hat{D}_2'(\beta\sqrt{\tau}) \, |0\rangle_{1'} |0\rangle_{2'} \tag{39}$$

since the input vacuum $|0\rangle_1 |0\rangle_2$ maps to the output vacuum $|0\rangle_{1'} |0\rangle_{2'}$.

We now take the limits. We have a highly excited coherent state, i.e. $|\beta| \to \infty$. The beam splitter is almost transparent, i.e. $\tau \to 1$. Their products stay constant-sized, i.e. $|\beta|\sqrt{1-\tau} \to$ const. In this limit, the displacements on mode $2'$ become $\hat{D}_2'(0)\hat{D}_2'(\beta\sqrt{\tau})$, which becomes independent of α and comes out of the integral, and so the output states becomes a simple product state. The remaining state in mode $1'$ becomes

$$\begin{aligned} &\frac{1}{\pi} \int d^2\alpha \, \langle\alpha|\psi\rangle \, \hat{D}_1'(\alpha) \, \hat{D}_1'(i\beta\sqrt{1-\tau}) \, |0\rangle_{1'} \\ =&\frac{1}{\pi} \int d^2\alpha \, \langle\alpha|\psi\rangle \, \hat{D}_1'(i\beta\sqrt{1-\tau}) \, |\alpha\rangle_{1'} \\ =&\hat{D}_1'(i\beta\sqrt{1-\tau}) \, |\psi\rangle \end{aligned} \tag{40}$$

which is the target state $|\psi\rangle$ acted by a displacement operator!

Since we are free to choose the exact value of β (which is complex) and τ by choosing the coherent state and the beam splitter parameters, we can achieve any displacement amount $i\beta\sqrt{1-\tau}$ in the output mode $1'$. As for the output mode $2'$, it can simply be discarded. Like the case in homodyne measurement, a phase shifter can be placed after the coherent state laser source to change the phase of β.

2.5 The Squeezer

In processes where two photons are created and two photons are destroyed, the Hamiltonian will contain quadratic ladder operator terms [7, 8, 9]. For example, in degenerate parametric amplification, a pump photon is split into a signal and a idler photon, both with half the pump photon's frequency. Neglecting the free evolution and assuming the pump field is approximately unchanged in time (the so-called "parametric approximation"; this can be achieved by using a strong coherent source [8]), the Hamiltonian of such processes have the form

$$\hat{H} = i\hbar\frac{\kappa}{2}(\hat{a}^{\dagger 2}e^{i\theta} - \hat{a}^2 e^{-i\theta}) \tag{41}$$

where θ is the phase of the pump field (adjustable by a phase shifter), and κ is a clumped parameter absorbing all the necessary dimensions like the magnitude of the pump and the susceptibility of the medium. The Hamiltonian (41) describes the amplification of the signal mode $\hat{a}$ at half the pump frequency. We claim that the signal mode will become squeezed by this Hamiltonian's time evolution.

For an intuitive argument, let us imagine the simple case of $\theta = 0$. The signal's mode evolves via the Heisenberg equation of motion [14]

$$\begin{aligned}\frac{d}{dt}\hat{a}(t) &= \frac{1}{i\hbar}[\hat{a}(t), \hat{H}] = \frac{\kappa}{2}[\hat{a}(t), \hat{a}^{\dagger 2}(t)] \\ &= \kappa\hat{a}^{\dagger}(t)\end{aligned} \tag{42}$$

whose solution is

$$\hat{a}(t) = \hat{a}(0)\cosh(\kappa t) + \hat{a}^{\dagger}(0)\sinh(\kappa t) \tag{43}$$

since

$$\frac{d}{dt}\hat{a}(t) = \kappa[\hat{a}(0)\sinh(\kappa t) + \hat{a}^{\dagger}(0)\cosh(\kappa t)] = \kappa\hat{a}^{\dagger}(t) \tag{44}$$

Casting (43) into the position and momentum quadratures gives

$$\begin{aligned}(\hat{X}+i\hat{P})(t) &= (\hat{X}+i\hat{P})(0)\,\frac{e^{\kappa t}+e^{-\kappa t}}{2} + (\hat{X}-i\hat{P})(0)\,\frac{e^{\kappa t}-e^{-\kappa t}}{2} \\ &= \hat{X}(0)\,e^{\kappa t} + i\hat{P}(0)\,e^{-\kappa t}\end{aligned} \tag{45}$$

We see that the signal mode's position expands as $\hat{X}(t) = \hat{X}(0)\,e^{\kappa t}$, and its momentum shrinks as $\hat{P}(t) = \hat{P}(0)\,e^{-\kappa t}$. Therefore, in time their respective variances [3] grow as $e^{2\kappa t}$ for the position and shrink as $e^{-2\kappa t}$ for the momentum. In other words, the uncertainty product $\Delta\hat{X}\Delta\hat{P}$ stays constant in time, but the uncertainty in one quadrature is decreasing, whereas the uncertainty in the other one in increasing. This is the signature of a squeezed state! The effect of the time evolution of the parametric amplification Hamiltonian (41) is that the signal mode becomes squeezed, with the amount of squeezing being κt, a dimensionless effective interaction time.

More generally, including the pump phase θ, since the squeezing Hamiltonian (41) does not contain explicit time dependence, its time evolution is thus [14]

$$\hat{U}(t) = \exp\!\left(-\frac{i}{\hbar}\hat{H}t\right) = \exp\!\left(\frac{\kappa}{2}(\hat{a}^{\dagger 2}e^{i\theta} - \hat{a}^2 e^{-i\theta})\,t\right) \tag{46}$$

Denote $\xi = -\kappa t e^{i\theta}$, $\xi^* = -\kappa t e^{-i\theta}$. The time evolution operator thus becomes the squeezing operator

$$\hat{U}(t) = \exp\!\left(\frac{1}{2}(\hat{a}^2\xi^* - \hat{a}^{\dagger 2}\xi)\right) = \hat{S}(\xi) \tag{47}$$

Its effects on the quadratures are given by (Appendix A)

$$\hat{S}^\dagger(\xi)\,\hat{a}\,\hat{S}(\xi) = \cosh(\kappa t)\,\hat{a} + e^{i\theta}\sinh(\kappa t)\,\hat{a}^\dagger \tag{48}$$

The pump phase θ can be tuned to control the squeezing axis. From equation (17) we have

$$\begin{aligned}\hat{X}^{(\theta)} + i\hat{P}^{(\theta)} &= (\cos\theta\hat{X} + \sin\theta\hat{P}) + i(-\sin\theta\hat{X} + \cos\theta\hat{P}) \\ &= (\cos\theta - i\sin\theta)\hat{X} + (\sin\theta + i\cos\theta)\hat{P} \\ &= e^{-i\theta}\hat{X} + i(-i\sin\theta + \cos\theta)\hat{P} \\ &= e^{-i\theta}(\hat{X} + i\hat{P}) = e^{-i\theta}\hat{a}\end{aligned} \tag{49}$$

[3] Reminder: the variance of an operator $\hat{A}$ is $\left\langle(\Delta\hat{A})^2\right\rangle = \left\langle\hat{A}^2\right\rangle - \left\langle\hat{A}\right\rangle^2$.

We can balance the phases between $\hat{a}$ and $\hat{a}^\dagger$ in (48) by looking at the $\theta/2$-phased quadratures.

$$\begin{aligned}
&\hat{S}^\dagger(\xi)\,(\hat{X}^{(\theta/2)} + i\hat{P}^{(\theta/2)})\,\hat{S}(\xi) \\
&= \hat{S}^\dagger(\xi)\,e^{-i\theta/2}\hat{a}\,\hat{S}(\xi) \\
&= e^{-i\theta/2}\cosh(\kappa t)\,\hat{a} + e^{i\theta/2}\sinh(\kappa t)\,\hat{a}^\dagger \\
&= e^{-i\theta/2}\,\frac{e^{\kappa t}+e^{-\kappa t}}{2}\,\hat{a} + e^{i\theta/2}\,\frac{e^{\kappa t}-e^{-\kappa t}}{2}\,\hat{a}^\dagger \\
&= e^{\kappa t}\,\frac{e^{-i\theta/2}\hat{a} + e^{i\theta/2}\hat{a}^\dagger}{2} + e^{-\kappa t}\,\frac{e^{-i\theta/2}\hat{a} - e^{i\theta/2}\hat{a}^\dagger}{2} \\
&= e^{\kappa t}\hat{X}^{(\theta/2)} + ie^{-\kappa t}\hat{P}^{(\theta/2)}
\end{aligned} \tag{50}$$

where we used the form (15) of the phase-ful quadratures. Since the squeeze operator $\hat{S}(\xi)$ is the time evolution operator of our Hamiltonian, we see that in time, the $\theta/2$-phased position quadrature and its uncertainty grows as $e^{\kappa t}$, and the momentum ones shrink as $e^{-\kappa t}$, which is the behavior of a general squeezed state. By controlling the pump phase θ via a phase shifter, and controlling the effective squeezing interaction time κt, we can perform a squeeze of an arbitrary amount about an arbitrary axis on the signal state.

2.6 Summary

Operation	Phase Space Operator	Circuit Symbol	Physical Implementation
Phase Shifter	$\hat{R}(\theta) = \exp\left(i\theta\hat{a}^\dagger\hat{a}\right)$ $\hat{R}^\dagger(\theta)\,\hat{a}\,\hat{R}(\theta) = \hat{a}e^{i\theta}$		A length of optical fibre [8]; or a thermo-optic phase shifter [12].
Displacement Operator	$\hat{D}(\alpha)$ $= \exp\left(\alpha\hat{a}^\dagger - \alpha^*\hat{a}\right)$ $\hat{D}^\dagger(\alpha)\,\hat{a}\,\hat{D}(\alpha)$ $= \hat{a} + \alpha$		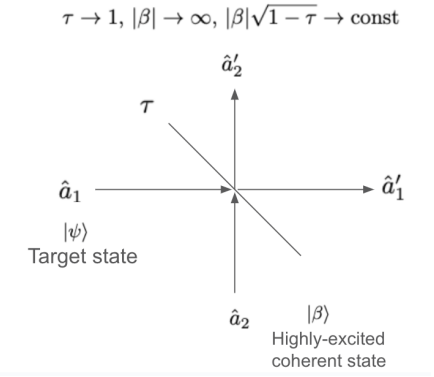
Squeezer	$\hat{S}(\xi)$ $= \exp\left(\frac{\hat{a}^2\xi^* - \hat{a}^{\dagger 2}\xi}{2}\right)$ $\hat{S}^\dagger(\xi)\,\hat{a}\,\hat{S}(\xi)$ $= \cosh(\kappa t)\,\hat{a}$ $\quad + e^{i\theta}\sinh(\kappa t)\,\hat{a}^\dagger$ $\xi = -\kappa t e^{i\theta}$		Processes involving the creation and destruction of two photons, e.g. degenerate parametric amplification [7, 8, 9]. The signal mode has the Hamiltonian $\hat{H} = i\hbar\frac{\kappa}{2}(\hat{a}^{\dagger 2}e^{i\theta} - \hat{a}^2 e^{-i\theta})$ whose time evolution operator is just $\hat{U}(t) = \hat{S}(\xi)$
Quadrature Measurement	Projection onto the measured quadrature eigenstate	N.A.	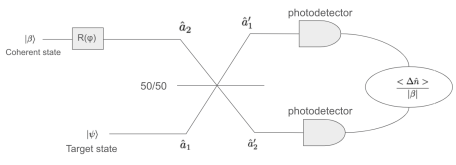

Table 1: Summary of basic optical operations and their implementations.

3 Optical Implementation of Gates in GKP Encoding

3.1 Overview of GKP Encoding

Now that we have learned how to implement the basic optical operations physically, let us discuss how these operations can build a quantum computer. Consequently, this will provide a scheme for physically implementing a quantum computer.

The GKP encoding was originally motivated by considering error corrections necessary for a quantum computer [1]. We will not be discussing error correction theory; rather, let us simply motivate the GKP states by thinking about the functionality of gates on qubits.

An encoding is a representation of a logical qubit state with a (or some) quantum state(s) of the physical implementation system. For example, a naive encoding could just be letting some atomic orbital represent the logical $|0\rangle_L$ state (we use subscript L to denote logical qubit states, and no subscripts for physical states), and some other atomic orbital represent $|1\rangle_L$. For light states, let us imagine simply using some coherent state $|\alpha_0\rangle$ to represent $|0\rangle_L$, and some other coherent state $|\alpha_1\rangle$ to represent $|1\rangle_L$.

The Pauli X gate, aka the not gate, brings $|0\rangle_L$ to $|1\rangle_L$. Therefore under out simple coherent state encoding, the physical implementation of the Pauli X gate is just the displacement operator $\hat{D}(\alpha_1 - \alpha_0)$, bringing $|\alpha_0\rangle$ to $|\alpha_1\rangle$. However, the X gate should also bring $|1\rangle_L$ to $|0\rangle_L$, but this displacement operator acting on $|\alpha_1\rangle$ brings it to $|2\alpha_1 - \alpha_0\rangle$, which is not the state representing $|0\rangle_L$.

This issue can be solved if instead of using a simple coherent state, we use a Dirac comb. The states we choose to encode the logical qubits in are

$$|\mu\rangle_L = \sum_{n=-\infty}^{\infty} \left|(2n+\mu)\sqrt{\pi}\right\rangle_x , \quad \mu \in \{0,1\} \tag{51}$$

where the subscript x denotes position eigenstates. These states are the GKP states [1, 2, 15]. Explicitly,

$$|0\rangle_L = \sum_{n=-\infty}^{\infty} \left|2n\sqrt{\pi}\right\rangle_x \tag{52}$$

$$|1\rangle_L = \sum_{n=-\infty}^{\infty} \left|(2n+1)\sqrt{\pi}\right\rangle_x \tag{53}$$

Their position-basis wavefunctions are two Dirac combs with periodic spacing $2\sqrt{\pi}$, and displaced with each other by $\sqrt{\pi}$.

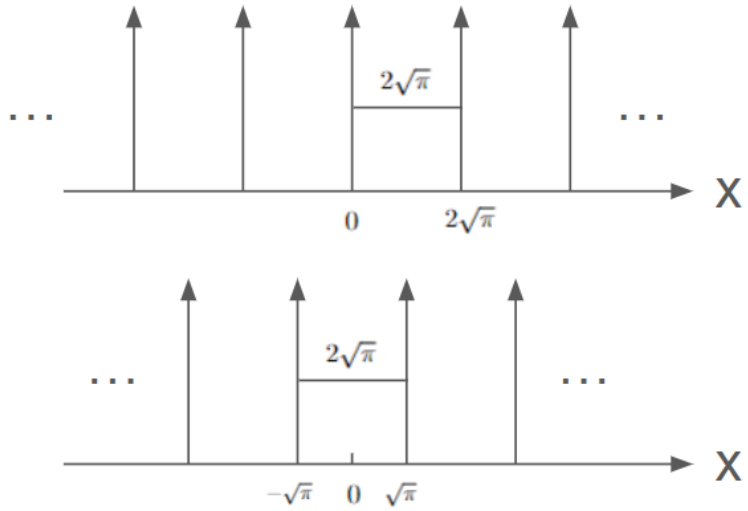

Figure 6: Position-basis ($\hat{X}$) wavefunctions of the GKP states $|0\rangle_L$ (top) and $|1\rangle_L$ (bottom).

The Pauli X gate in this encoding is obviously just the displacement operator $\hat{D}(\sqrt{\pi})$ (whose physical implementation we discussed earlier!), translating the wavefunction in position space by $\sqrt{\pi}$. Moreover, applying the X gate twice now corresponds to a translation of $2\sqrt{\pi}$, which brings both GKP states back to themselves, since they are $2\sqrt{\pi}$ periodic. This is the desired behavior of a not gate!

Qubit measurement is also easily supported by these encoding states: all we need to do is simply measure the position quadrature with homodyne measurement. If we measured a position that is an even multiple of $\sqrt{\pi}$, then we know we measured $|0\rangle_L$; and if an odd multiple of $\sqrt{\pi}$, then $|1\rangle_L$.

3.2 Wigner Functions of GKP States

To study these GKP states in more depth, the first order of business is to calculate the Wigner functions of the various GKP states. To illustrate the effect of some important Clifford gates, we will show the Wigner function of the six Pauli eigenstates [15].

Because Wigner function is not linear, i.e. Wigner function of a superposition is NOT the superposition of the constituent Wigner functions, we cannot just calculate the Wigner functions of $|0\rangle_L$ and $|1\rangle_L$ and form linear combinations from them for a general qubit state.

All we can do is directly plug a general qubit state [4]

$$|\Psi\rangle_L = \cos\left(\frac{\theta}{2}\right)|0\rangle_L + e^{i\phi}\sin\left(\frac{\theta}{2}\right)|1\rangle_L \tag{54}$$

$$\Psi(x) = \cos\left(\frac{\theta}{2}\right)\Psi_0(x) + e^{i\phi}\sin\left(\frac{\theta}{2}\right)\Psi_1(x) \tag{55}$$

into the definition of the Wigner function (20). Here $\Psi_j(x) = \langle x|j\rangle_L$ is the position basis wavefunction of GKP state $|j\rangle_L$.

It is clear that all terms in the Wigner function will be of the following form

$$W_{jk}(x,p) = \int dx' e^{ipx'}\Psi_j^*(x+x'/2)\Psi_k(x-x'/2) \tag{56}$$

which we now compute. Start by plugging in the Dirac comb wavefunctions (51), and repeatedly using $\delta(ax) = \delta(x)/|a|$,

$$\begin{aligned}
W_{jk}(x,p) &= \int dx' e^{ipx'}\left[\sum_s^\infty \delta\Big(x+x'/2-\sqrt{\pi}(j+2s)\Big)\right]\left[\sum_t^\infty \delta\Big(x-x'/2-\sqrt{\pi}(k+2t)\Big)\right] \\
&= \sum_{st}^\infty \int dx' e^{ipx'}\delta\Big(x+x'/2-\sqrt{\pi}(j+2s)\Big)2\delta\Big(2x-x'-2\sqrt{\pi}(k+2t)\Big) \\
&= \sum_{st}^\infty 2\exp\Big(ip(2x-2\sqrt{\pi}(k+2t))\Big)\delta\Big(x+\frac{2x-2\sqrt{\pi}(k+2t)}{2}-\sqrt{\pi}(j+2s)\Big) \\
&= \sum_{st}^\infty 2\exp\Big(i2p(x-\sqrt{\pi}(k+2t))\Big)\delta\Big(2x-\sqrt{\pi}(k+2t+j+2s)\Big) \\
&= \sum_{st}^\infty \exp\Big(i2p(x-\sqrt{\pi}(k+2t))\Big)\delta\Big(x-\frac{\sqrt{\pi}}{2}(k+2t+j+2s)\Big)
\end{aligned} \tag{57}$$

Change dummy variables as $t \to t-s$ (which still goes to infinity):

$$\begin{aligned}
(57) &= \sum_{st}^\infty \exp\Big(i2p(x-\sqrt{\pi}(k+2t-2s))\Big)\delta\Big(x-\frac{\sqrt{\pi}}{2}(k+2t+j)\Big) \\
&= \sum_{st}^\infty \exp\Big(i2p\sqrt{\pi}2s\Big)\underbrace{\exp\Big(i2p[x-\sqrt{\pi}(k+2t)]\Big)\delta\Big(x-\frac{\sqrt{\pi}}{2}(k+2t+j)\Big)}_{=\exp\left(i2p\left[\frac{\sqrt{\pi}}{2}(k+2t+j)-\sqrt{\pi}(k+2t)\right]\right)\delta\left(x-\frac{\sqrt{\pi}}{2}(k+2t+j)\right)} \\
&= \sum_{st}^\infty \exp\Big(i2p\sqrt{\pi}2s\Big)\exp\Big(ip\sqrt{\pi}(j-k-2t)\Big)\delta\Big(x-\frac{\sqrt{\pi}}{2}(k+2t+j)\Big)
\end{aligned} \tag{58}$$

[4] For those who are comfortable with such things, we are using the same angles θ and ϕ for a two-level system on a Bloch sphere.

where we used the cute little fact $f(x)\delta(x-x') = f(x')\delta(x-x')$.

Now the only term that contains s is the $\exp(i2p\sqrt{\pi}2s)$. This sum can be easily performed, since we know the Fourier series coefficients of a delta comb with period d is $\sum_s \delta(q-sd) = \sum_s \frac{1}{d}\exp(2\pi iqs/d)$ (see any introductory text on Fourier transform and signal analysis, e.g. Oppenheim and Willsky, example 3.8). Thus with $d = \sqrt{\pi}/2$,

$$\sum_s \exp\big(i2p\sqrt{\pi}2s\big) = \sum_s \frac{\sqrt{\pi}}{2}\delta\bigg(p - s\frac{\sqrt{\pi}}{2}\bigg) \tag{59}$$

Therefore

$$\begin{aligned}(58) &= \sum_{st}^{\infty} \frac{\sqrt{\pi}}{2}\,\delta\bigg(p - s\frac{\sqrt{\pi}}{2}\bigg)\exp\bigg(ip\sqrt{\pi}(j-k-2t)\bigg)\delta\bigg(x - \frac{\sqrt{\pi}}{2}(k+2t+j)\bigg) \\ &= \sum_{st}^{\infty} \frac{\sqrt{\pi}}{2}\,\delta\bigg(p - s\frac{\sqrt{\pi}}{2}\bigg)\underbrace{\exp\bigg(i(s\sqrt{\pi}/2)\sqrt{\pi}(j-k-2t)\bigg)}_{=\exp(i\pi s(j-k-2t)/2) = (-1)^{s(j-k-2t)/2}}\delta\bigg(x - \frac{\sqrt{\pi}}{2}(k+2t+j)\bigg)\end{aligned} \tag{60}$$

And thus we have arrived at our result

$$\begin{aligned}W_{jk}(x,p) &= \int dx' e^{ipx'}\Psi_j^*(x+x'/2)\Psi_k(x-x'/2) \\ &= \frac{\sqrt{\pi}}{2}\sum_{st}^{\infty}(-1)^{s(j-k-2t)/2}\,\delta\bigg(p - s\frac{\sqrt{\pi}}{2}\bigg)\delta\bigg(x - \frac{\sqrt{\pi}}{2}(k+2t+j)\bigg)\end{aligned} \tag{61}$$

Perhaps at this point we should emphasize the obvious fact that $W_{00}(x,p)$ and $W_{11}(x,p)$ (i.e. when $j=k$) are just the Wigner functions of $|0\rangle_L$ and $|1\rangle_L$ (with some factors of 2π in front), respectively.

The Wigner function of basis GKP state $|j\rangle_L, j = 0, 1$, is

$$\boxed{W_j(x,p) = \frac{1}{4\sqrt{\pi}}\sum_{st}^{\infty}(-1)^{st}\,\delta\bigg(p - s\frac{\sqrt{\pi}}{2}\bigg)\delta\bigg(x - \sqrt{\pi}(t+j)\bigg)} \tag{62}$$

Let us analyze what this Wigner function looks like. It is zero everywhere except where both deltas are non-zero, which occur at discrete points. In other words, we have a (square) lattice of delta spikes. Denote this lattice by $(l,m) \equiv (x = ld, p = md)$, with $d = \sqrt{\pi}/2$ being the lattice spacing, and l, m both integers.

Focus on $j = 0$ (since $j = 1$ will just be $j = 0$ shifted in x to the right by $\sqrt{\pi} = 2d$). We see that the non-zero spikes in the x direction have a step size of $\sqrt{\pi} = 2d$, and those in the p direction have a step size of just $\sqrt{\pi}/2 = d$.

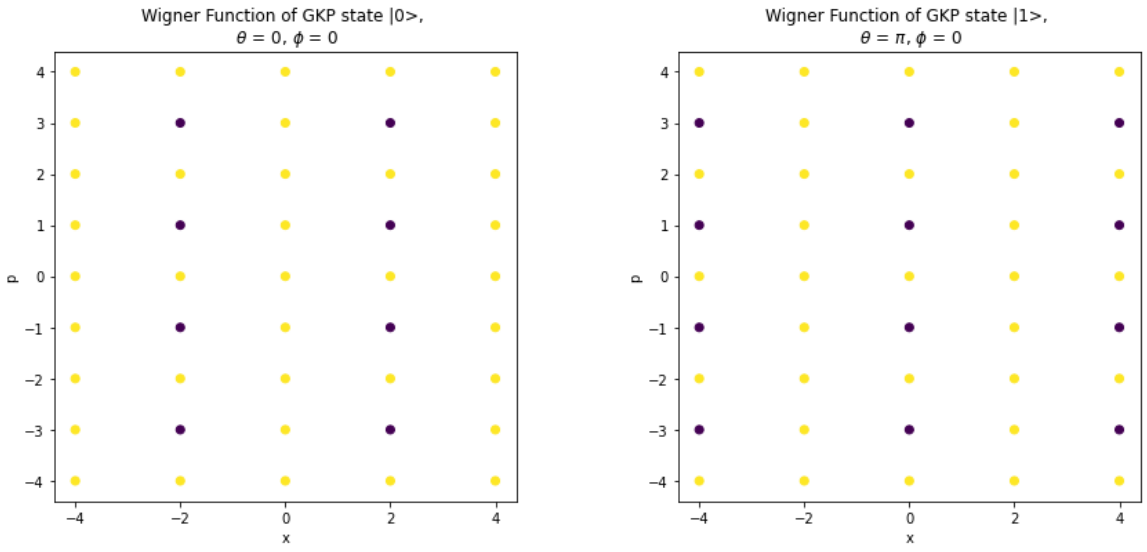

Figure 7: Wigner functions of $|0\rangle_L$ and $|1\rangle_L$. Purple points represent negative delta spikes, yellow points represent positive delta spikes. The grid spacing (i.e. one unit length on the plot) of both x and p axes is $d = \sqrt{\pi}/2$.

For the sign of the non-zero delta spikes, notice that the integer combination st in (62) will be odd only when both s and t are odd. This occurs one-fourth of the time, so one-fourth of all the non-zero delta spikes will be negative, with the remaining spikes positive. The negative spikes are at odd s in the p direction with spacing d, so every other p coordinate, and odd t in the x direction with spacing $2d$, so every fourth x coordinate. The Wigner functions of $|0\rangle_L$ and $|1\rangle_L$ are plotted and shown in figure 7. Notice for $j = 0$, i.e. $|0\rangle_L$, the lattice point $(l, m) = (2, 1)$ is negative, since it corresponds to $(x, p) = (\sqrt{\pi}, \sqrt{\pi}/2)$, which is $t = 1, s = 1$ in (62).

The Wigner function of a general GKP qubit state (55), parameterized by the Bloch angles θ, ϕ, is

$$\begin{aligned}
W(\theta,\phi;x,p) &= \frac{1}{2\pi}\int dx' e^{ipx'}\,\Psi^*(x+\frac{x'}{2})\,\Psi(x-\frac{x'}{2}) \\
&= \frac{1}{2\pi}\int dx' e^{ipx'}\left[\cos\left(\frac{\theta}{2}\right)\Psi_0^*(x+\frac{x'}{2}) + e^{-i\phi}\sin\left(\frac{\theta}{2}\right)\Psi_1^*(x+\frac{x'}{2})\right] \\
&\qquad\qquad \times\left[\cos\left(\frac{\theta}{2}\right)\Psi_0(x-\frac{x'}{2}) + e^{i\phi}\sin\left(\frac{\theta}{2}\right)\Psi_1(x-\frac{x'}{2})\right] \\
&= \cos^2\left(\frac{\theta}{2}\right)W_0(x,p) + \sin^2\left(\frac{\theta}{2}\right)W_1(x,p) \\
&+ \frac{1}{2\pi}\cos\left(\frac{\theta}{2}\right)\sin\left(\frac{\theta}{2}\right)\left[e^{i\phi}W_{01}(x,p) + e^{-i\phi}W_{10}(x,p)\right]
\end{aligned} \tag{63}$$

Using (61) for the cross term,

$$
\begin{aligned}
(63) &= \cos^2\left(\frac{\theta}{2}\right) W_0(x,p) + \sin^2\left(\frac{\theta}{2}\right) W_1(x,p) \\
&+ \frac{1}{4\sqrt{\pi}} \cos\left(\frac{\theta}{2}\right) \sin\left(\frac{\theta}{2}\right) \left[e^{i\phi} \sum_{st}^{\infty} (-1)^{s(-1-2t)/2}\, \delta\left(p - s\frac{\sqrt{\pi}}{2}\right) \delta\left(x - \frac{\sqrt{\pi}}{2}(1+2t)\right) \right. \\
&\left. + e^{-i\phi} \sum_{st}^{\infty} (-1)^{s(1-2t)/2}\, \delta\left(p - s\frac{\sqrt{\pi}}{2}\right) \delta\left(x - \frac{\sqrt{\pi}}{2}(1+2t)\right) \right] \\
&= \cos^2\left(\frac{\theta}{2}\right) W_0(x,p) + \sin^2\left(\frac{\theta}{2}\right) W_1(x,p) \\
&+ \frac{1}{8\sqrt{\pi}} \sin\theta \sum_{st}^{\infty} (-1)^{st} \left[e^{i\phi}(-1)^{s/2} + e^{-i\phi}(-1)^{-s/2} \right] \delta\left(p - s\frac{\sqrt{\pi}}{2}\right) \delta\left(x - \frac{\sqrt{\pi}}{2}(1+2t)\right)
\end{aligned}
\tag{64}
$$

since $(-1)^{s(-1-2t)/2} = (-1)^{-s/2-st} = (-1)^{st+s/2}$, and $(-1)^{s(1-2t)/2} = (-1)^{s/2-st} = (-1)^{st-s/2}$.

Noticing that $e^{i\phi}(-1)^{s/2} + e^{-i\phi}(-1)^{-s/2} = e^{i\phi}e^{i\pi s/2} + e^{-i\phi}e^{-i\pi s/2} = 2\cos(\phi + \pi s/2)$, we arrive at the Wigner function for a general GKP state:

For GKP state

$$
|\Psi\rangle_L = \cos\left(\frac{\theta}{2}\right) |0\rangle_L + e^{i\phi} \sin\left(\frac{\theta}{2}\right) |1\rangle_L \tag{65}
$$

the Wigner function is

$$
\begin{aligned}
W(\theta,\phi;x,p) &= \cos^2\left(\frac{\theta}{2}\right) W_0(x,p) + \sin^2\left(\frac{\theta}{2}\right) W_1(x,p) \\
&+ \frac{1}{4\sqrt{\pi}} \sin\theta \sum_{st}^{\infty} (-1)^{st} \cos\left(\phi + \pi\frac{s}{2}\right) \delta\left(p - s\frac{\sqrt{\pi}}{2}\right) \delta\left(x - \frac{\sqrt{\pi}}{2}(1+2t)\right)
\end{aligned}
\tag{66}
$$

where $W_0(x,p)$ and $W_1(x,p)$ are the Wigner functions of $|0\rangle_L$ and $|1\rangle_L$, as given by (62) and shown in figure 7.

With some straightforward analysis (see Appendix B), we see that the Wigner function of a general GKP state is also a lattice of delta spikes, just like W_0 and W_1. It is the superposition of infinitely many delta spikes, labeled by $(l, m) \equiv (x = ld, p = md)$, with $d = \sqrt{\pi}/2$ being the lattice spacing, and l, m both integers. The coefficient of each (l, m) delta spike is given by table 2 (without an overall $1/4\sqrt{\pi}$ factor).

	$l = 4u$	$l = 4u + 1$	$l = 4u + 2$	$l = 4u + 3$
$m = 4v$	$\cos^2\theta/2 + \sin^2\theta/2$	$\sin\theta\cos\phi$	$\sin^2\theta/2 + \cos^2\theta/2$	$\sin\theta\cos\phi$
$m = 4v + 1$	$\cos^2\theta/2 - \sin^2\theta/2$	$-\sin\theta\sin\phi$	$\sin^2\theta/2 - \cos^2\theta/2$	$\sin\theta\sin\phi$
$m = 4v + 2$	$\cos^2\theta/2 + \sin^2\theta/2$	$-\sin\theta\cos\phi$	$\sin^2\theta/2 + \cos^2\theta/2$	$-\sin\theta\cos\phi$
$m = 4v + 3$	$\cos^2\theta/2 - \sin^2\theta/2$	$\sin\theta\sin\phi$	$\sin^2\theta/2 - \cos^2\theta/2$	$-\sin\theta\sin\phi$

Table 2: Superposition coefficients of each delta spike for the Wigner function of a general GKP state $\cos(\theta/2)\,|0\rangle_L + \exp(i\phi)\sin(\theta/2)\,|1\rangle_L$. The lattice integers (l, m) have a period of 4, and the unit cell thus contains 16 lattice points. In this table u, v are both integers; they are simply there to indicate the modular group represented by the table cell entry. The table omits an overall factor of $1/4\sqrt{\pi}$.

The lattice is periodic with period $4d$ in both directions. In the table we keep sums of the form $\cos^2(\cdot) + \sin^2(\cdot)$ instead of writing 1 to blend them into the rest of the table.

With these coefficients, we can easily plot the Wigner function of the six logical Pauli eigenstates. Let us denote them by

$$\begin{aligned} |z+\rangle &= |0\rangle_L & |z-\rangle &= |1\rangle_L \\ |x+\rangle &= \frac{|0\rangle_L + |1\rangle_L}{\sqrt{2}} & |x-\rangle &= \frac{|0\rangle_L - |1\rangle_L}{\sqrt{2}} \\ |y+\rangle &= \frac{|0\rangle_L + i\,|1\rangle_L}{\sqrt{2}} & |y-\rangle &= \frac{|0\rangle_L - i\,|1\rangle_L}{\sqrt{2}} \end{aligned} \tag{67}$$

Their respective Bloch angles can be easily obtained, and their GKP delta spike coefficients can then be calculated. Their Wigner functions are shown in figure 8.

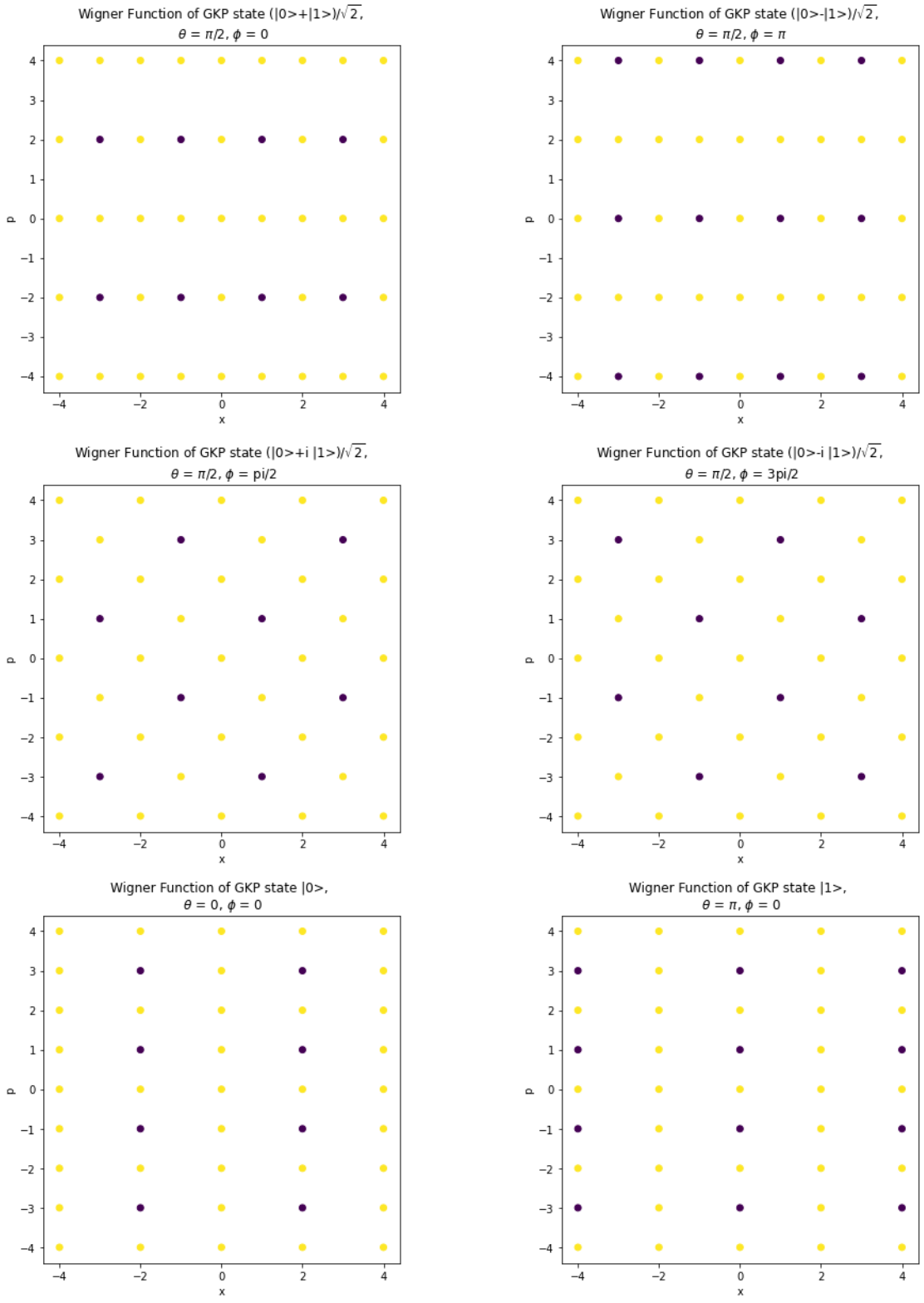

Figure 8: Wigner functions of all six Pauli eigenstates in GKP encoding. Purple points represent negative delta spikes, yellow points represent positive delta spikes. The grid spacing (i.e. one unit length on the plot) of both x and p axes is $d = \sqrt{\pi}/2$.

3.3 The Hadamard and Pauli Gates [2]

Inspecting the Wigner functions, we see that Pauli X and Z gates on GKP qubits correspond to displacements along X and P by $\sqrt{\pi}$, respectively. The Pauli X gate takes $|1\rangle_L$ to $|0\rangle_L$ and vice versa, so it corresponds to the transformation between $|z+\rangle$ and $|z-\rangle$. which is a horizontal displacement of $2d = \sqrt{\pi}$. The Pauli Z gate flips the sign of $|1\rangle_L$, which maps $|x+\rangle$ (and $|y+\rangle$) to $|x-\rangle$ (and $|y-\rangle$), and vice versa. In phase space this is a vertical displacement of $2d = \sqrt{\pi}$. Physically, both of these gates can be implemented by the displacement operator discussed in chapter 2.

The Hadamard gate is simply a $\pi/2$ rotation in phase space, implementable by a phase-shifter. The Hadamard gate takes $|z+\rangle$ to $|x+\rangle$, and the rotation is obvious.

3.4 The Phase Gate [2]

Another important quantum gate is the phase gate

$$\hat{S} = \begin{pmatrix} 1 & 0 \\ 0 & i \end{pmatrix} = (\hat{Z})^{1/2} \tag{68}$$

which takes $|1\rangle_L$ to $i\,|1\rangle_L$, and hence takes $|x+\rangle$ to $|y+\rangle$, and $|y+\rangle$ to $|x-\rangle$. Putting on our hat of geometrical wisdom and imagination, we see that the corresponding transformation in phase space is a vertical shear $X \to X$, $P \to P - X$. For example, the point $(X, P) = (1, 2)$ in $|x+\rangle$ (the first "upper right" negative spike) maps to $(1, 2-1) = (1, 1)$ in $|y+\rangle$, and $(-1, -2)$ to $(-1, -1)$.

How to physically implement a shear in phase space? In fact, a shear can be decomposed into operations we already covered. Define the **shear operator** in optical phase space

$$\hat{P}(s) = \exp\left(i\, s\hat{X}^2\right) \tag{69}$$

(recall that the phase space quadratures are dimensionless in our convention). The effect of this operator on the quadratures are (Appendix A)

$$\hat{P}^\dagger(s)\, \hat{X}\, \hat{P}(s) = \hat{X} \tag{70}$$

$$\hat{P}^\dagger(s)\, \hat{P}\, \hat{P}(s) = \hat{P} + s\hat{X} \tag{71}$$

Obviously the shear operator shears the momentum quadrature and leaves the position untouched. Choosing $s = -1$ would produce the logical GKP phase gate.

The shear operator can be decomposed into a rotation and a squeeze. In fact, such gate decomposition of more complicated gates into basic Gaussian gates is possible for a wide range of gates, including the optical CX and CZ gates [16, 17]. The general theory and procedures to perform such decompositions are sufficiently well-understood. Here let us focus on the shear operator. The decomposition of the shear operator is given by [2, 16, 17]

$$\hat{P}(s) = \hat{R}(\theta)\hat{S}(re^{i\phi}) \tag{72}$$

or, denoting the squeeze parameter with $re^{i\phi} = \xi$ (a different convention than the one we used when discussing the squeeze operator with parametric processes, though this should raise no axiety):

$$\exp\left(is\hat{X}^2\right) = \exp\left(i\theta\hat{a}^\dagger\hat{a}\right)\exp\left(\frac{1}{2}(\hat{a}^2\xi^* - \hat{a}^{\dagger 2}\xi)\right) \tag{73}$$

with $\cosh(r) = \sqrt{1+(s/2)^2}$, $\tan\theta = s/2$, $\phi = -\text{sign}(s)\pi/2 - \theta$.

We now verify this claim. To establish (73), first notice that a non-infinitesimal shear can be built up from infinitesimal shears:

$$\hat{P}(s_1+s_2) = e^{i(s_1+s_2)\hat{X}^2} = e^{is_1\hat{X}^2 + is_2\hat{X}^2} = e^{is_1\hat{X}^2}e^{is_2\hat{X}^2} = \hat{P}(s_1)\hat{P}(s_2) \tag{74}$$

where we secretly used the BCH formula when the exponents commute. Thus it suffices to prove (73) with small s. Since $\tan\theta = s/2$, we also have small θ. Also $\cosh(r) = \sqrt{1+(s/2)^2}$ means $\cosh(r) \approx 1$, so r is small as well. Physically, this says a small shear only needs a small rotation and a small squeeze, which is perfectly reasonable.

(73) will need to be thrown into the BCH formula. The commutator between the exponents is

$$\begin{aligned}
[i\theta\hat{a}^\dagger\hat{a}, \frac{1}{2}(\hat{a}^2\xi^* - \hat{a}^{\dagger 2}\xi)] &= \frac{1}{2}i\theta\left(\xi^*[\hat{a}^\dagger\hat{a}, \hat{a}^2] - \xi[\hat{a}^\dagger\hat{a}, \hat{a}^{\dagger 2}]\right) \\
&= \frac{1}{2}i\theta(\xi^*(-2\hat{a}^2) - \xi(2\hat{a}^{\dagger 2})) \\
&= -i\theta(\xi^*\hat{a}^2 + \xi\hat{a}^{\dagger 2})
\end{aligned} \tag{75}$$

Higher orders of commutators would thus include higher orders of θ and $\xi = re^{i\phi}$. Since we have small θ, we only keep the first order commutator. BCH formula thus gives

$$\begin{aligned}
\exp\left(i\theta\hat{a}^\dagger\hat{a}\right)\exp\left(\frac{1}{2}(\hat{a}^2\xi^* - \hat{a}^{\dagger 2}\xi)\right) &= \exp\left(i\theta\hat{a}^\dagger\hat{a} + \frac{1}{2}(\hat{a}^2\xi^* - \hat{a}^{\dagger 2}\xi) - i\frac{\theta}{2}(\xi^*\hat{a}^2 + \xi\hat{a}^{\dagger 2})\right) \\
&= \exp\left(is\hat{X}^2\right)
\end{aligned} \tag{76}$$

Plugging in $\xi = re^{i\phi}$ and $\hat{a} = \hat{X} + i\hat{P}$, after some algebra, the gigantic exponent becomes

$$\exp\Bigg(\hat{X}^2\Big[-r\sin(\phi)i+i\theta-i\theta r\cos(\phi)\Big] \\ +\hat{P}^2\Big[r\sin(\phi)i+i\theta+i\theta r\cos(\phi)\Big] \\ +(\hat{X}\hat{P}+\hat{P}\hat{X})\Big[ir\cos(\phi)-i\theta r\sin(\phi)\Big] \\ -\frac{1}{2}i\theta\Bigg)=\exp\Big(is\hat{X}^2\Big) \tag{77}$$

Equating corresponding coefficients of $\hat{X}$ and $\hat{P}$, we have

$$\theta - r\sin(\phi) - \theta r\cos(\phi) = s \tag{78}$$
$$\theta + r\sin(\phi) + \theta r\cos(\phi) = 0 \tag{79}$$
$$r\cos(\phi) - \theta r\sin(\phi) = 0 \tag{80}$$
$$\frac{1}{2}\theta = 0 \tag{81}$$

(81) is automatically satisfied since we are looking at small θ. Adding (78) and (79) gives $\theta = s/2$, which recovers $\tan\theta = s/2$ in small s.

(80) gives $1-\theta\tan\phi = 0$, so $\tan\theta\tan\phi = 1$ with small θ. This says θ and ϕ are symmetric about the $y=x$ (or $y=-x$) line in the unit circle plane, or $\phi+\theta = \pm\pi/2$ depending on the quadrant. This recovers $\phi = -\text{sign}(s)\pi/2 - \theta$.

With small θ, so $\phi \approx \pm\pi/2$, so $\cos(\phi)\approx 0$ and $\sin(\phi)\approx\pm 1$. (78) can be massaged as $\theta - s = r(\sin(\phi)+\theta\cos(\phi)) \approx \pm r$. With $\theta = s/2$, this gives $s/2 \approx \pm r$, so $r^2 \approx (s/2)^2$.

Now, $\cosh(r) = \sum_n r^{2n}/(2n)! \approx 1 + r^2/2$ for small r. On the other hand, using $\sqrt{1+\epsilon}\approx 1+\epsilon/2$ for small ϵ, we have $\sqrt{1+(s/2)^2}\approx 1+(s/2)^2/2$. With $r^2\approx(s/2)^2$, we recover $\cosh(r) = \sqrt{1+(s/2)^2}$.

(73) is now proved for an infinitesimal shear, and thus a "full" shear. Physically, (73) says the GKP phase gate can be implemented by a squeezer followed by a phase shifter.

3.5 The *CNOT* Gate [2]

With a similar decomposition procedure [16, 17], we can implement the $CNOT$ gate with single-mode squeezers and beam splitters. Denote the beam splitter operator by

$$\hat{B}(\theta,\phi) = \exp\Big(\theta(e^{i\phi}\hat{a}_1\hat{a}_2^\dagger - e^{-i\phi}\hat{a}_1^\dagger\hat{a}_2)\Big) \tag{82}$$

We leave the reader to verify that the action of the beam splitter operator on the quadratures are

$$\begin{cases} \hat{B}^\dagger(\theta,\phi)\hat{X}_1\hat{B}(\theta,\phi) = \hat{X}_1\cos(\theta) - \sin(\theta)\Big[\hat{X}_2\cos(\phi) + \hat{P}_2\sin(\phi)\Big] \\ \hat{B}^\dagger(\theta,\phi)\hat{P}_1\hat{B}(\theta,\phi) = \hat{P}_1\cos(\theta) - \sin(\theta)\Big[\hat{P}_2\cos(\phi) - \hat{X}_2\sin(\phi)\Big] \end{cases} \tag{83}$$

$$\begin{cases} \hat{B}^\dagger(\theta,\phi)\hat{X}_2\hat{B}(\theta,\phi) = \hat{X}_2\cos(\theta) + \sin(\theta)\Big[\hat{X}_1\cos(\phi) - \hat{P}_1\sin(\phi)\Big] \\ \hat{B}^\dagger(\theta,\phi)\hat{P}_2\hat{B}(\theta,\phi) = \hat{P}_2\cos(\theta) + \sin(\theta)\Big[\hat{P}_1\cos(\phi) + \hat{X}_1\sin(\phi)\Big] \end{cases} \tag{84}$$

In other words, the transmittivity and reflectivity amplitudes of the beam splitter are $t = \cos\theta$ and $r = e^{i\phi}\sin\theta$ respectively. Again this is a different beam splitter coefficient convention than the one in chapter 2, and again this should raise no anxiety for us.

The GKP $CNOT$ and CZ gates correspond to CX and CZ gates in the optical domain, respectively, since we already saw that a GKP Pauli X (Z) gate is a horizontal (vertical) phase space displacement. It can be shown, via a similar procedure to that of the shearer, that the optical CX gate can be broken down into a pair of single-mode squeezers between two beam-splitters, and optical CZ gate can be broken into a CX gate sandwiched between two phase shifters on the target mode [16, 17]:

$$\hat{CX}(s) \equiv \int dx\,|x\rangle\langle x| \otimes \hat{D}(sx) = \exp\Big(-2is\hat{X}_1\otimes\hat{P}_2\Big) \tag{85}$$

$$= \hat{B}(\theta+\pi/2,0)[\hat{S}(r)\otimes\hat{S}(-r)]\hat{B}(\theta,0) \tag{86}$$

$$\hat{CZ}(s) \equiv \iint dxdy\, e^{2isxy}\,|x,y\rangle\langle x,y| = \exp\Big(2is\hat{X}_1\otimes\hat{X}_2\Big) \tag{87}$$

$$= (\hat{1}\otimes\hat{R}(\pi/2))\,\hat{CX}(s)\,(\hat{1}\otimes\hat{R}^\dagger(\pi/2)) \tag{88}$$

where $\sin(2\theta) = -1/\cosh(r)$, $\cos(2\theta) = -\tanh(r)$, $\sinh(r) = -s/2$.

4 Preparation of GKP states with Gaussian Boson Sampling (GBS)

Now that we have covered how photonic optical circuit elements can be used to implement qubit gates with GKP states, let us briefly review how these GKP states can be physically produced in the first place. The preparation procedure utilizes a technique called Gaussian Boson Sampling (GBS) [10, 3, 4, 5].

4.1 Rationale of GBS

The basic principle of GBS is very simple. Back in section 2.1.4 we formulated optical devices as input-output (unitary) devices. Imagine an optical device with n input ports and n output ports. The inputs can be displaced squeezed states. At the outputs, we perform a Fock-basis measurement on all but one of the ports, and leave one output port unmeasured. The state at the remaining unmeasured port is the prepared output state of the GBS scheme. This technique works because the interferometer will entangle all the input ports, so measurement results at some output ports can effect the post-measurement state at other output ports.

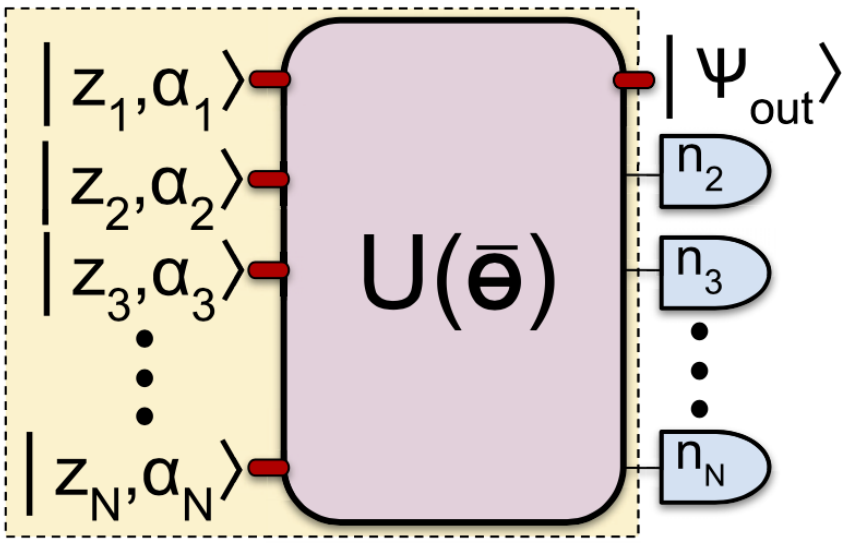

Figure 9: The general GBS scheme. The device $U(\theta)$, e.g. an interferometer, takes in displaced squeezed states $|z_i, \alpha_i\rangle$. At all but one output ports we perform Fock basis measurements with photon-number-resolving-detectors. The state at the remaining output port is the single-mode output state we have prepared. Figure is taken from [3].

In fact, with this scheme we can effectively prepare *any* single-state we wish, not just limited to GKP states.

Because the preparation depends on the Fock measurement results at the other outputs, preparation of any target state is inherently probabilistic. Given the input squeeze and displacement parameters z_i, α_i and the interferometer parameters θ, we can calculate the probability of preparing a desired state [10].

As a trivial example, the garden-variety 50-50 beam splitter is actually a GBS device:

$$\begin{pmatrix} \hat{a}_2 \\ \hat{a}_3 \end{pmatrix} = \frac{1}{\sqrt{2}} \begin{pmatrix} 1 & i \\ i & 1 \end{pmatrix} \begin{pmatrix} \hat{a}_0 \\ \hat{a}_1 \end{pmatrix} \tag{89}$$

$$\begin{pmatrix} \hat{a}_0 \\ \hat{a}_1 \end{pmatrix} = \frac{1}{\sqrt{2}} \begin{pmatrix} 1 & -i \\ -i & 1 \end{pmatrix} \begin{pmatrix} \hat{a}_2 \\ \hat{a}_3 \end{pmatrix} \tag{90}$$

Let's say the input state is $|0\rangle_0 |1\rangle_1 = \hat{a}_1^\dagger |0\rangle_0 |0\rangle_0$ (not a squeezed displaced vacuum, but the rationale is the same). The output state across all output ports is

$$\frac{1}{\sqrt{2}}(i\hat{a}_2^\dagger + \hat{a}_3^\dagger) |0\rangle_2 |0\rangle_3 = \frac{1}{\sqrt{2}}(i |1\rangle_2 |0\rangle_3 + |0\rangle_2 |1\rangle_3) \tag{91}$$

which is now entangled. To prepare $|0\rangle$ (or $|1\rangle$) at port 2, we need to measure 1 (or 0) photon at port 3. This measurement result, of course, is probabilistic.

The expression for this probability is in general quite complicated [10]. For a desired state we want to prepare, we need to design the set of parameters z_i, α_i, θ, and the corresponding measurement result needed at the measured ports. We then wish to maximize the probability of obtaining these measurement results.

In practice, this is a question of parameter-tuning optimization. The exact form of the probability is thus not necessary. The standard practice is to use machine learning to tune these parameters [3, 4, 5], which we do not go into here. Here it suffices to note that the algorithm for finding these parameters are quite mature.

4.2 An Example Preparation of GKP Zero State

We now showcase how the above GBS scheme can be used to prepared the GKP $|0\rangle_L$ state. This example, along with all the figures, is quoted from [3].

The ideal GKP $|0\rangle_L$ state is an infinite delta comb, and is thus unphysical. The doable thing in the lab is (a) give it an overall Gaussian envelope so it doesn't stretch out infinitely in space, and (b) represent each delta spike with narrow, tall Gaussians. This approximate GKP state can in principal be built from an infinite superposition of Fock basis states, but for simplicity let us only use $|0\rangle, |2\rangle$ and $|4\rangle$. Note that $|0\rangle_L$ is even.

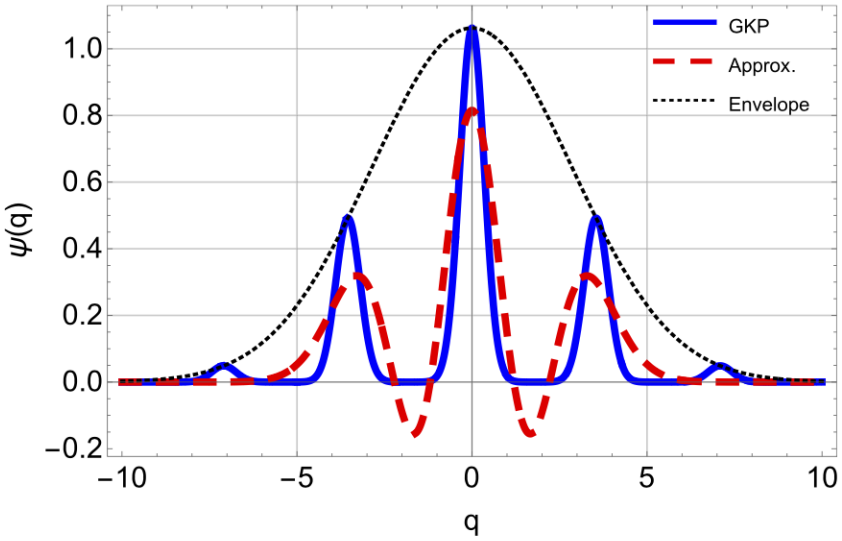

Figure 10: Position basis wavefunction of GKP zero state. The blue solid line is the GKP state approximated by a Gaussian envelop and spikes as tiny Gaussians. The red dashed line is approximating the blue solid line with only wavefunctions of Fock states $|0\rangle$, $|2\rangle$ and $|4\rangle$.

The red dashed line is the wavefunction of the state

$$\hat{S}(0.294)(0.669\,|0\rangle - 0.216\,|2\rangle + 0.711\,|4\rangle) \equiv |target\rangle \tag{92}$$

We wish to prepare $|target\rangle$ with GBS. Of course, these numbers are fine-tuned parameters from the discussed machine learning procedure.

We prepare $|target\rangle$ by measuring two modes of a three-mode GBS scheme. The three input squeezing parameters are $(z_1, z_2, z_3) = (1.33803, 0.101223, 0.0994552)$. The interferometer

unitary is

$$U = \begin{pmatrix} 0 & -0.704006i & -0.710195 \\ 0.707107 & u_{22} & u_{33} \\ -0.707107 & u_{22} & u_{33} \end{pmatrix}$$
$$u_{22} = 0.355097 - 0.355098i, \quad u_{33} = 0.352003 + 0.352002i \tag{93}$$

With these parameters, measuring photon numbers $(2, 2)$ at ports 2 and 3 will produce $|target\rangle$ at port 1. This measurement probability is approximately 1.1%.

The interferometer unitary can then be decomposed into basic devices like beam splitters and phase shifters.

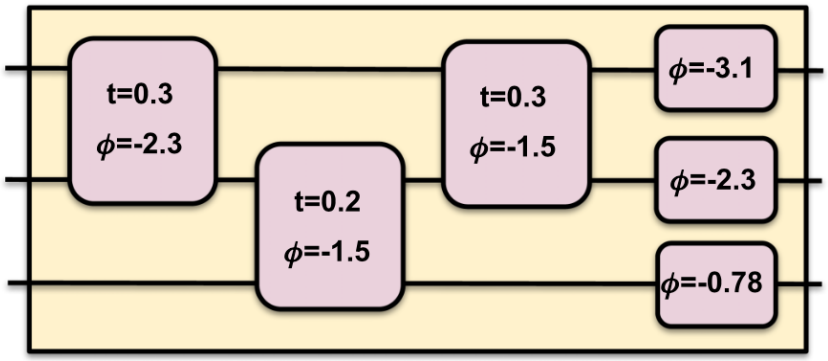

Figure 11: Decomposing the interferometer unitary (93) into beam splitters and phase shifters. The first operator depicts a beam splitter of transmission t preceded by a phase rotation by ϕ in the first mode alone. The operator denoted by only a phase angle is the standard phase rotation gate.

5 Conclusion

We have performed a gentle yet lightspeed literature review of photonic quantum computing with GKP states. We looked at the GKP encoding, and discussed how a photonic quantum computer with GKP encoding can in principle be built in the lab with optical circuit elements. We then looked at how these GKP states can be physically produced. In principle, after reading this document, one should be able to go into the lab and build a photonic quantum computer!

For further reading, we suggest all the cited sources. Emphasizing on the device physics of photonic quantum computers, we especially recommend [2] and [4].

We purposefully avoided discussing error correction in this literature review, as we wished to focus on the device physics. For a discussion on the error correction aspects of the GKP encoding (which are where its true powers shine), see [1] and [2].

Appendix A

Operator expansion theorem [8] states that for any two operators $\hat{A}, \hat{B}$, we have

$$e^{\hat{B}}\,\hat{A}\,e^{-\hat{B}} = \sum_{n=0}^{\infty} \frac{1}{n!}\,[\underbrace{\hat{B},[\hat{B},...,[\hat{B}}_{n},\hat{A}\,\underbrace{]...]]}_{n}$$
$$= \hat{A} + [\hat{B},\hat{A}] + \frac{1}{2!}[\hat{B},[\hat{B},\hat{A}]] + ... \tag{94}$$

Useful commutators:

$$[\hat{a}^\dagger,\hat{a}^2] = [\hat{a}^\dagger,\hat{a}]\hat{a} + \hat{a}[\hat{a}^\dagger,\hat{a}] = -2\hat{a} \tag{95}$$
$$[\hat{a},\hat{a}^{\dagger 2}] = [\hat{a},\hat{a}^\dagger]\hat{a}^\dagger + \hat{a}^\dagger[\hat{a},\hat{a}^\dagger] = 2\hat{a}^\dagger \tag{96}$$
$$[\hat{a}^\dagger\hat{a},\hat{a}] = [\hat{a}^\dagger,\hat{a}]\hat{a} + \hat{a}^\dagger[\hat{a},\hat{a}] = -\hat{a} \tag{97}$$
$$[\hat{a}^\dagger\hat{a},\hat{a}^2] = [\hat{a}^\dagger,\hat{a}^2]\hat{a} = -2\hat{a}^2 \tag{98}$$
$$[\hat{a}^\dagger\hat{a},\hat{a}^{\dagger 2}] = \hat{a}^\dagger[\hat{a},\hat{a}^{\dagger 2}] = 2\hat{a}^{\dagger 2} \tag{99}$$

- Equation (22), displacement operator $\hat{D}(\alpha) = \exp\big(\alpha\hat{a}^\dagger - \alpha^*\hat{a}\big)$:

$$[\alpha^*\hat{a} - \alpha\hat{a}^\dagger,\hat{a}] = -\alpha[\hat{a}^\dagger,\hat{a}] = \alpha \tag{100}$$

The first order commutator is a number, so all higher commutators vanish:

$$\hat{D}^\dagger(\alpha)\,\hat{a}\,\hat{D}(\alpha) = \hat{D}(-\alpha)\,\hat{a}\,\hat{D}(\alpha)$$
$$= \exp\big(-\alpha\hat{a}^\dagger + \alpha^*\hat{a}\big)\,\hat{a}\,\exp\big(\alpha\hat{a}^\dagger - \alpha^*\hat{a}\big)$$
$$= \hat{a} + \alpha \tag{101}$$

- Equation (30), rotation operator $\hat{R}(\theta) = \exp\big(i\theta\hat{a}^\dagger\hat{a}\big)$:

$$n = 1: \quad [-i\theta\hat{a}^\dagger\hat{a},\hat{a}] = -i\theta[\hat{a}^\dagger\hat{a},\hat{a}] = i\theta\hat{a} \tag{102}$$
$$n = 2: \quad [-i\theta\hat{a}^\dagger\hat{a},[-i\theta\hat{a}^\dagger\hat{a},\hat{a}]] = [-i\theta\hat{a}^\dagger\hat{a},i\theta\hat{a}] = (i\theta)^2\hat{a} \tag{103}$$
$$n = k: \quad [-i\theta\hat{a}^\dagger\hat{a},(n=k-1)] = [-i\theta\hat{a}^\dagger\hat{a},(i\theta)^{k-1}\hat{a}] = (i\theta)^k\hat{a} \tag{104}$$

$$\hat{R}^\dagger(\theta)\,\hat{a}\,\hat{R}(\theta) = \exp\big(-i\theta\hat{a}^\dagger\hat{a}\big)\,\hat{a}\,\exp\big(i\theta\hat{a}^\dagger\hat{a}\big)$$
$$= \hat{a} + (i\theta)\hat{a} + (i\theta)^2\hat{a}/2! + ...$$
$$= \hat{a}e^{i\theta} \tag{105}$$

- Equation (48), squeeze operator $\hat{S}(\xi) = \exp\left(\frac{1}{2}(\hat{a}^2\xi^* - \hat{a}^{\dagger 2}\xi)\right)$:

With $\hat{B} = -\frac{1}{2}(\hat{a}^2\xi^* - \hat{a}^{\dagger 2}\xi)$, we have

$[\hat{B}, \hat{a}] = \frac{1}{2}\xi\,[\hat{a}^{\dagger 2}, \hat{a}] = -\xi\hat{a}^\dagger, \quad [\hat{B}, \hat{a}^\dagger] = -\frac{1}{2}\xi^*\,[\hat{a}^2, \hat{a}^\dagger] = -\xi^*\hat{a}$

$$n = 1: \quad [\hat{B}, \hat{a}] = -\xi\hat{a}^\dagger \tag{106}$$

$$n = 2: \quad [\hat{B}, [\hat{B}, \hat{a}]] = [\hat{B}, -\xi\hat{a}^\dagger] = |\xi|^2\hat{a} \tag{107}$$

$$n = 3: \quad [\text{... 3 layers ...}] = [\hat{B}, |\xi|^2\hat{a}] = -\xi|\xi|^2\hat{a}^\dagger \tag{108}$$

$$n = 4: \quad [\text{... 4 layers ...}] = [\hat{B}, -\xi|\xi|^2\hat{a}^\dagger] = |\xi|^4\hat{a} \tag{109}$$

$$n = 2k: \quad [\text{... an even number of layers ...}] = |\xi|^{2k}\hat{a} \tag{110}$$

$$n = 2k+1: \quad [\text{... an odd number of layers ...}] = -\xi|\xi|^{2k}\hat{a}^\dagger \tag{111}$$

Therefore, with $\xi = -\kappa t e^{i\theta}$,

$$\begin{aligned}
\hat{S}^\dagger(\xi)\,\hat{a}\,\hat{S}(\xi) &= e^{\hat{B}}\,\hat{a}\,e^{-\hat{B}} \\
&= \sum_{n=0}^{\infty}\frac{1}{(2n)!}[\underbrace{\hat{B}, [\hat{B}, ..., [\hat{B}}_{2n}, \hat{a}\,\underbrace{]...]]}_{2n} + \frac{1}{(2n+1)!}[\underbrace{\hat{B}, [\hat{B}, ..., [\hat{B}}_{2n+1}, \hat{a}\,\underbrace{]...]]}_{2n+1} \\
&= \sum_{n=0}^{\infty}\frac{1}{(2n)!}|\xi|^{2n}\hat{a} + \frac{1}{(2n+1)!}(-\xi|\xi|^{2n})\hat{a}^\dagger \\
&= \left(\sum_{n=0}^{\infty}\frac{(\kappa t)^{2n}}{(2n)!}\hat{a}\right) + \left(\sum_{n=0}^{\infty}\frac{(\kappa t)^{2n+1}}{(2n+1)!}e^{i\theta}\hat{a}^\dagger\right) \\
&= \cosh(\kappa t)\,\hat{a} + e^{i\theta}\sinh(\kappa t)\,\hat{a}^\dagger
\end{aligned} \tag{112}$$

- Equation (70), shear operator $\hat{P}(s) = \exp\left(i\,s\hat{X}^2\right)$:

$$n = 1: \quad [-i\,s\hat{X}^2, \hat{a}] = -i\,s([\hat{X}, \hat{a}]\hat{X} + \hat{X}[\hat{X}, \hat{a}]) = i\,s\hat{X} \tag{113}$$

$$n \geq 2: \text{ all higher commutators vanish since } \hat{X} \text{ commutes with itself} \tag{114}$$

where we used $[\hat{X}, \hat{a}] = [\hat{X}, \hat{X} + i\hat{P}] = i[\hat{X}, \hat{P}] = i(i/2) = -1/2$.

$$\begin{aligned}
\hat{P}^\dagger(s)\,\hat{a}\,\hat{P}(s) &= \exp\left(-i\,s\hat{X}^2\right)\,\hat{a}\,\exp\left(i\,s\hat{X}^2\right) \\
&= \hat{a} + i\,s\hat{X}
\end{aligned} \tag{115}$$

Taking the real and imaginary parts gives equation (70) in the main text.

Appendix B

$$W_j(x,p) = \frac{1}{4\sqrt{\pi}} \sum_{st}^{\infty} (-1)^{st}\, \delta\left(p - s\frac{\sqrt{\pi}}{2}\right) \delta\left(x - \sqrt{\pi}(t+j)\right)$$

$$W(\theta,\phi;x,p) = \cos^2\left(\frac{\theta}{2}\right) W_0(x,p) + \sin^2\left(\frac{\theta}{2}\right) W_1(x,p)$$
$$+ \frac{1}{4\sqrt{\pi}} \sin\theta \sum_{st}^{\infty} (-1)^{st} \cos\left(\phi + \pi\frac{s}{2}\right) \delta\left(p - s\frac{\sqrt{\pi}}{2}\right) \delta\left(x - \frac{\sqrt{\pi}}{2}(1+2t)\right)$$

Delta spike lattice: $(l,m) \equiv (x = ld, p = md)$, with $d = \sqrt{\pi}/2$ being the lattice spacing, and l, m both integers.

It is immediately clear that $W(\theta,\phi;x,p)$ is periodic in both x and p with a period of $4d = 2\sqrt{\pi}$, since the transformations $x \to x - 2\sqrt{\pi}$ and $p \to p - 2\sqrt{\pi}$ will correspond to $t \to t+2$ and $s \to s+4$, respectively, both leaving $W(\theta,\phi;x,p)$ invariant. Let us adopt the shorthand "$l = 1$" to mean "$l = 4u+1$", i.e. it suffices to indicate the modular group mod 4 of l and m, since the repeating unit cell of the lattice has 16 points.

The two self terms' contribution are immediately clear from figure 7:

	$l=0$	$l=1$	$l=2$	$l=3$
W_0	1	0	1 if m even, -1 if m odd	0
W_1	1 if m even, -1 if m odd	0	1	0

Table 3: Self-term coefficients for GKP Wigner function.These coefficients will multiply $\cos^2(\theta/2)$ for W_0 and $\sin^2(\theta/2)$ for W_1.

For the cross term, the $\delta(p - (\sqrt{\pi}/2)s) = \delta(p - ds)$ visits every integer m, and the $\delta(x - d(1+2t))$ visits only odd l (obviously m is identified with s, and l is identified with $(2t+1)$). Therefore the even l values are completely determined by the self terms. Table 3 thus produce the columns $l = 4u$ and $l = 4u+2$ in table 2.

First look at the $\cos(\phi + \pi s/2)$. Since every integer m is visited, we need all 4 alternatives for this coefficient. Using $\cos(\phi + m\pi/2) = \cos\phi\cos(m\pi/2) - \sin\phi\sin(m\pi/2)$, we have

m	$\cos(m\pi/2)$	$\sin(m\pi/2)$	$\cos(\phi + m\pi/2)$
0	1	0	$\cos\phi$
1	0	1	$-\sin\phi$
2	-1	0	$-\cos\phi$
3	0	-1	$\sin\phi$

The extra $(-1)^{st}$ factor: since only odd l are visited, and since in the sum this odd l appears as $(2t+1)$, so when t is odd, $(2t+1) = (2(2u+1)+1) = (4u+3)$. Thus the (odd m, $l = 4u+3$) entries will pick up an extra minus sign.

Remembering that the cross terms have an overall $\sin\theta$, we arrive at the columns $l = 4u+1$ and $l = 4u+3$ in table 2.

References

[1] Daniel Gottesman, Alexei Kitaev, and John Preskill. "Encoding a qubit in an oscillator". In: *Phys. Rev. A* 64 (1 2001), p. 012310. DOI: 10.1103/PhysRevA.64.012310. URL: https://link.aps.org/doi/10.1103/PhysRevA.64.012310.

[2] J. Eli Bourassa et al. "Blueprint for a Scalable Photonic Fault-Tolerant Quantum Computer". In: *Quantum* 5 (Feb. 2021), p. 392. ISSN: 2521-327X. DOI: 10.22331/q-2021-02-04-392. URL: https://doi.org/10.22331/q-2021-02-04-392.

[3] Daiqin Su, Casey R. Myers, and Krishna Kumar Sabapathy. "Conversion of Gaussian states to non-Gaussian states using photon-number-resolving detectors". In: *Phys. Rev. A* 100 (5 Nov. 2019), p. 052301. DOI: 10.1103/PhysRevA.100.052301. URL: https://link.aps.org/doi/10.1103/PhysRevA.100.052301.

[4] Ilan Tzitrin et al. "Progress towards practical qubit computation using approximate Gottesman-Kitaev-Preskill codes". In: *Phys. Rev. A* 101 (3 Mar. 2020), p. 032315. DOI: 10.1103/PhysRevA.101.032315. URL: https://link.aps.org/doi/10.1103/PhysRevA.101.032315.

[5] Krishna Kumar Sabapathy et al. "Production of photonic universal quantum gates enhanced by machine learning". In: *Phys. Rev. A* 100 (1 July 2019), p. 012326. DOI: 10.1103/PhysRevA.100.012326. URL: https://link.aps.org/doi/10.1103/PhysRevA.100.012326.

[6] M. A. Nielsen and I. L. Chuang. *Quantum Computation and Quantum Information*. Cambridge University Press, 2010. ISBN: 9781107002173.

[7] Samuel L. Braunstein and Peter van Loock. "Quantum information with continuous variables". In: *Rev. Mod. Phys.* 77 (2 June 2005), pp. 513–577. DOI: 10.1103/RevModPhys.77.513. URL: https://link.aps.org/doi/10.1103/RevModPhys.77.513.

[8] C. Gerry and P. Knight. *Introductory Quantum Optics*. Cambridge University Press, 2004. ISBN: 9780511791239.

[9] G. Grynberg, A. Aspect, and C. Fabre. *Introduction to Quantum Optics: From the Semi-classical Approach to Quantized Light*. Cambridge University Press, 2010. ISBN: 9780511778261.

[10] Craig S. Hamilton et al. "Gaussian Boson Sampling". In: *Phys. Rev. Lett.* 119 (17 Oct. 2017), p. 170501. DOI: 10.1103/PhysRevLett.119.170501. URL: https://link.aps.org/doi/10.1103/PhysRevLett.119.170501.

[11] W.B. Case. "Wigner Functions and Weyl Transforms for Pedestrians". In: *Am. J. Phys.* 76 (2008), p. 937. DOI: 10.1119/1.2957889. URL: http://www.stat.physik.uni-potsdam.de/~pikovsky/teaching/stud_seminar/Wigner_function.pdf.

[12] Shahryar Sabouri et al. “Thermo Optical Phase Shifter With Low Thermal Crosstalk for SOI Strip Waveguide”. In: *IEEE Photonics Journal* 13.2 (2021), pp. 1–12. DOI: 10.1109/JPHOT.2021.3056902.

[13] Matteo G.A. Paris. “Displacement operator by beam splitter”. In: *Physics Letters A* 217.2 (1996), pp. 78–80. ISSN: 0375-9601. DOI: https://doi.org/10.1016/0375-9601(96)00339-8. URL: https://www.sciencedirect.com/science/article/pii/0375960196003398.

[14] J. J. Sakurai and Jim Napolitano. *Modern Quantum Mechanics, 2nd Edition*. Cambridge University Press, 2017. ISBN: 9781108422413.

[15] L. García-Álvarez, A. Ferraro, and G. Ferrini. “From the Bloch Sphere to Phase-Space Representations with the Gottesman–Kitaev–Preskill Encoding”. In: *International Symposium on Mathematics, Quantum Theory, and Cryptography*. Ed. by Tsuyoshi Takagi et al. Singapore: Springer Singapore, 2021, pp. 79–92. ISBN: 978-981-15-5191-8. DOI: 10.1007/978-981-15-5191-8_9.

[16] Nathan Killoran et al. “Strawberry Fields: A Software Platform for Photonic Quantum Computing”. In: *Quantum* 3 (Mar. 2019), p. 129. ISSN: 2521-327X. DOI: 10.22331/q-2019-03-11-129. URL: https://doi.org/10.22331/q-2019-03-11-129.

[17] *Strawberry Fields Photonic Gate Documentation*. https://strawberryfields.ai/photonics/conventions/gates.html.